

## CHAPTER 1

## INTRODUCTION

Partial differential equations (PDEs) [1, 2] are important tools for the modeling of physics. They arise in numerous fields, see, for instance, the Poisson equation [3, 4], elasticity equations [5, 6] in continuum mechanics, the wave equation [7] in acoustics, Maxwell's equations [8] in electromagnetism, the Schrödinger equation [9] in quantum mechanics, magnetohydrodynamics (MHD) [10, 11] equations in plasma physics, Stokes equations [12], Euler equations [13, 14] and Navier-Stokes equations [15–17] in fluid dynamics and many more.

These equations can be broken down into two types of relations, constitutive relations and topological relations. Constitutive relations are also called constitutive laws. A typical constitutive relation describes the relation between two variables connected by a material parameter. Such a relation essentially is a scientific hypothesis and can only be verified to a certain degree through experiments. While a topological relation usually refers to a conservation law which is considered to be a fundamental law of nature. We take the Poisson equation as an example. The Poisson equation arises in many subjects, like fluid dynamics [18], heat transfer [19], electromagnetism [20], gravity [21], etc. It is an elliptic partial differential equation of the form

$$-\nabla \cdot (k\nabla\varphi) = f,$$

where  $\varphi$  and  $f$  are both scalar fields and  $k$  refers to a material property. If we introduce an intermediate variable  $\mathbf{u} = k\nabla\varphi$ , the Poisson equation can be broken down into a mixed formulation written as

$$\begin{aligned}\mathbf{u} &= k\nabla\varphi, \\ \nabla \cdot \mathbf{u} &= -f.\end{aligned}$$

If the Poisson equation is used to model a heat diffusion, the first relation, namely the gradient relation, then represents a constitutive law, Fourier's law, which relates the heat flux  $\mathbf{u}$  to the temperature  $\varphi$  subject to a material property  $k$ , the thermal conductivity of the material. And the second relation, the divergence relation, simply implies the fundamental conservation law of energy, i.e., that the local net heat flux must be equal to the heat generated or absorbed by the source term,  $f$ . As a second example, if the Poisson equation models a potential flow in porous medium, the gradient relation then represents a constitutive relation — Darcy's law which relates the flow velocity field,  $\mathbf{u}$ , to the flow potential,  $\varphi$ , subject to a material property  $k$ , the permeability of the medium. And the divergence relation reflects the fundamental conservation law of mass stating that the local net mass flux is equal to the mass generated or absorbed by the source term,  $f$ . In practice, a constitutive relation may already contain a certain amount of error.

For instance, the measurement of the thermal conductivity of a material or the permeability of a porous medium comes with a certain measurement error. However, the topological relation which stands for the topological essence of physics does not contain such an error. Apart from the constitutive and topological relations, there are other structures, like symmetries and invariants, embedded in PDEs.

For a particular problem, it is generally difficult to find the analytical solutions of the PDEs. An alternative approach is doing a simulation with a numerical method to find an approximate solution [22, 23]. Common numerical methods can be classified into finite difference methods (FDM) [8, 24], finite volume methods (FVM) [15, 25] and finite element methods (FEM) [26–30]. For example, given a well-posed Poisson problem in a porous medium, using the conventional first order finite element method, we can find a numerical solution of the velocity field  $\mathbf{u}$ , denoted by  $\mathbf{u}^h$ , i.e.,

$$\mathbf{u}^h \approx \mathbf{u},$$

which is a linear combination of piece-wise linear functions. However, if we check the conservation of mass for the numerical solution  $\mathbf{u}^h$ , we will find that it is only satisfied approximately, i.e.,

$$\nabla \cdot \mathbf{u}^h \approx 0,$$

where we have assumed that there is no source term anywhere, namely  $f = 0$ . The exact conservation of mass,  $\nabla \cdot \mathbf{u} = 0$ , can only be approached when we refine the simulation to the limit, which is not feasible because of the limited computational power. We can interpret this by saying that artificial mass is generated during the numerical simulation. In other words, the structure which prevents the unphysical artificial mass, the conservation of mass embedded by the relation  $\nabla \cdot \mathbf{u} = 0$ , is not preserved by the numerical method.

Besides methods like the aforementioned conventional finite element method which fail to maintain these structures of PDEs in the solutions, there are numerical methods designed to take one or some structures as strong constraints such that they can be strictly satisfied by the solutions. Such methods are called *structure-preserving* or *mimetic* methods. The feature of being structure-preserving leads to extra physical compatibility, and also benefits the method generally in the aspects of accuracy and, more importantly, stability [31]. Therefore, structure-preserving methods have become a research topic of great interest. Among the various structure-preserving methods, there is the *mimetic spectral element method* (MSEM) [32–34], an arbitrary-order structure-preserving method.

**Complement 1.1** Complements are provided at

[PhD thesis complements (ptc)] [www.mathischeap.com/contents/LIBRARY/ptc](http://www.mathischeap.com/contents/LIBRARY/ptc).

They serve as a library and contain additional material such as instructions and well-documented scripts that could help readers (especially the new researchers) to better understand the MSEM and its extensions and to more quickly build their own efficient programs.

## 1.1 A literature study of structure-preserving methods

Back in the 1960s, methods which employ staggered meshes were proposed. Among them there are the method proposed by Harlow and Welch [35] and the Smagorinsky-Lilly method firstly introduced by Smagorinsky [36] and then developed by Lilly [37]. These methods discuss the conservation and mathematical properties of the problems and could be considered as the original mimetic methods.

In the 1970s, Tonti [38–41] introduced a classification scheme for the basic physical quantities and theories and revealed the analogies between *algebraic topology* [42, 43] and *differential*

*geometry* [44–47]. In this scheme, physical variables are associated with not only points but also other elementary geometric elements of higher dimensions, such as lines, surfaces and volumes. In algebraic topology, more specifically the theory of cell-complexes, these geometric elements are called *k-cells* with *k* being the dimension of the geometric elements. On a grid, the numbered and oriented *k-cells* form a *k-chain*. The association between a *k-chain* and a *k-cochain* which can be regarded as the degrees of freedom of a discrete differential *k-form* then can be established [48]. Tonti’s work, from a more geometric point of view, gives a novel and robust tool to understand different physical theories, to analyze the mathematical structure embedded in them and to design numerical methods, especially structure-preserving methods [49].

Before the work of Tonti, Whitney formulated an interpolation between flat cochains and differential forms for a proof in his geometric integration theory [50]. These forms initially were not used for numerical methods until Dodziuk [51] generalized these ideas onto manifolds, named them *Whitney forms*, and used them in a finite difference approach to the Hodge theory of harmonic forms in 1974 [52]. Around the same time, in the field of finite element methods, a new branch called *mixed finite element methods* was proposed and developed by Brezzi, Raviart, Thomas, Nédélec, Douglas et al., [53–57]. These newly developed *mixed elements* turn out to be closely related to the Whitney forms [58, 59]. For this reason Whitney forms, in a finite element setting, are also called *Whitney elements* which were then used in the field of computational electromagnetics by Bossavit in the late 1980s [60–62]. Instead of conventional scalar and vector fields used in the mixed finite element methods, Bossavit used differential forms for the description and numerical modeling of physics, which was a great success and promoted the use of differential forms and Whitney forms in other fields. Bossavit’s work in computational electromagnetics is also recognized as a pioneering work in the structure-preserving or mimetic discretization community, and Whitney forms are also gradually known as finite elements for differential forms [52]. For more recent developments, we highlight the work on higher order Whitney forms [63, 64] and on Whitney forms for various cell shapes [65].

Although Tonti’s work shares some similar ideas with Whitney forms (and mixed elements) and partly contributed to Bossavit’s work [66–70], by the early 1990s, Whitney forms (and mixed elements) had become much more popular than Tonti’s work, unjustly as Bossavit said in [71]. Attempts were made to merge them in the same paper. Nevertheless, it is undeniable that both of them are important and useful tools for structure-preserving or mimetic methods.

The terminology mimetic discretization became well-known since the development of the mimetic finite difference (MFD) method. The method was called to be mimetic as it mimics some fundamental properties of mathematical and physical systems [72]. Driven by the idea that the discrete differential operators, such as gradient, curl and divergence, should be conservative such that they preserve some properties, like standard vector identities, symmetry, positive definiteness, of their continuous counterparts, Hyman and Scovel [73] proposed a mimetic finite difference approach based on the analogies between algebraic topology and differential forms in 1988. Later, a complete framework for the mimetic finite difference method was gradually established from the middle 1990s by Hyman, Shashkov, Lipnikov, Steinberg et al., see for example [74–79]. We emphasize [72] for a comprehensive review on the mimetic finite difference method. The virtual element method [80], a close variation of the mimetic finite difference method, can also be classified into this framework. For more application-oriented work on the mimetic finite difference method, we refer to, for example, [81, 82].

The popularity of exploring the usage of algebraic topology and differential forms for mimetic discretizations reached another level from the early 2000s. In the work of Bochev and Hyman [83], a more general framework that could be used to guide the development of mimetic discretization in any of finite difference, finite volume and finite element settings was constructed by extending the early work of Hyman and Scovel [73]. At the kernel of this framework, there

are two basic operations, the *reduction* and the *reconstruction*. On a domain of dimension  $n$ , the reduction operation maps differential  $k$ -forms ( $k \leq n$ ) onto  $k$ -cochains. These  $k$ -cochains are associated to  $k$ -chains which are part of a cell complex that tessellates the domain. The reconstruction operation, as a right inverse of the reduction, reconstructs the discrete differential  $k$ -forms from the  $k$ -cochains. Discrete operators like discrete inner product and discrete Hodge operator depend on the reconstruction, and, thus, for various choices of the reconstruction, different mimetic methods can arise.

In the same period, a mimetic discretization theory called the *discrete exterior calculus* (DEC) was developed by Hirani, Desbrun, Marsden et al. [84–87]. Sharing close ideas with the mimetic framework proposed by Bochev and Hyman, for example, in the sense of discrete operators, such as exterior derivative, codifferential and Hodge operator, the DEC provides a more geometric approach to address the topic. For a fully mimetic discrete vector calculus, we refer to the work of Robidoux and Steinberg [88]. For more investigations of mimetic methods in unstructured meshes, we refer to the work of Perot and his co-authors [89, 90].

Another important contribution called the *finite element exterior calculus* (FEEC) was made by Arnold, Falk and Winther [91–94] which forms an excellent foundation for the combination of mimetic ideas and finite element methods. The mimetic ideas can also be implemented in the *mimetic isogeometric analysis*, see for example the work of Evans, Hughes, Toshniwal and their co-authors [95, 96]. More investigations on mimetic discretization in the finite element setting include for example the work of Hiptmair [97, 98], Bonelle, Ern, Di Pietro et al., [99–101] and the MSEM.

The MSEM (which will be introduced comprehensively in Chapter 2) proposed by Gerritsma, Palha, Kreeft et al. [32–34] was inspired by many of the previously mentioned contributions among which the mimetic framework proposed by Bochev and Hyman, the discrete exterior calculus and the finite element exterior calculus are the most direct ones.

For more structure-preserving discretizations in various mathematical fields, see, for example, the work of Hairer, Lubich and Wanner on geometric numerical integration [102–104], [105–107] on mimetic variational approaches, and [108–111] on Hamiltonian systems.

## CHAPTER 2

## MIMETIC SPECTRAL ELEMENT METHOD

In this chapter, we introduce the MSEM which was firstly introduced using the mathematical language of differential forms, see [33, 34, 112]. Here we explain the method with the more conventional mathematical language, vector calculus, to provide another way of understanding the method for a larger audience.

For various applications of the MSEM, we refer to, for example, [3, 6, 12, 14, 17, 113–119].

## 2.1 The Poisson problem

As explained in the introduction chapter, the Poisson problem arises in many branches of physics and engineering, like fluid dynamics [18], heat transfer [19], electromagnetism [20], gravity [21], etc. It is governed by the Poisson equation, an elliptic partial differential equation, of the strong form<sup>1</sup>

$$-\nabla \cdot (k\nabla\varphi) = f,$$

where  $\varphi$  and  $f$  are both scalar fields and  $k$  refers to a material parameter. We consider a simply connected, bounded domain  $\Omega$  whose regular enough (Lipschitz continuous) boundary is denoted by  $\partial\Omega$ . The boundary  $\partial\Omega$  is split into two parts,  $\Gamma_\varphi$  and  $\Gamma_{\mathbf{u}}$ ,

$$\partial\Omega = \Gamma_\varphi \cup \Gamma_{\mathbf{u}}, \quad \Gamma_\varphi \cap \Gamma_{\mathbf{u}} = \emptyset, \quad \Gamma_\varphi \neq \emptyset.$$

Let the material parameter  $k$  and the scalar field  $f$  be known and boundary conditions  $\varphi = \hat{\varphi}$  and  $\mathbf{u} \cdot \mathbf{n} = \hat{u}$  be given on  $\Gamma_\varphi$  and  $\Gamma_{\mathbf{u}}$ , respectively. Note that we use  $\mathbf{n}$  to denote the outward unit normal vector. If we introduce an auxiliary variable  $\mathbf{u} = \nabla\varphi$ , a well-posed Poisson problem can be expressed in a mixed form,

$$\begin{aligned} (2.1a) \quad & \mathbf{u} = k\nabla\varphi && \text{in } \Omega, \\ (2.1b) \quad & \nabla \cdot \mathbf{u} = -f && \text{in } \Omega, \\ (2.1c) \quad & \varphi = \hat{\varphi} && \text{on } \Gamma_\varphi \\ (2.1d) \quad & \mathbf{u} \cdot \mathbf{n} = \hat{u} && \text{on } \Gamma_{\mathbf{u}}. \end{aligned}$$

<sup>1</sup>This form is strong in the sense that we have not applied any restriction to the spaces that the variables belong to.

Note that when  $\Gamma_\varphi = \emptyset$ , this problem is not well-posed. There is a singular mode in (2.1a). For example, if  $\varphi'$  solves the problem,  $\varphi = \varphi' + C$ , where  $C$  is an arbitrary constant<sup>2</sup>, also solves the problem.

## 2.2 The de Rham structure

### 2.2.1 Function spaces

We start with some basic concepts of Sobolev spaces [27, 120, 121] on which the de Rham complex will be built. The fundamental Sobolev space we will use in this chapter is the space of square integrable functions,

$$L^2(\Omega) := \{\varphi \mid \langle \varphi, \varphi \rangle_\Omega < +\infty\},$$

where  $\langle \cdot, \cdot \rangle_\Omega$  denotes the  $L^2$ -inner product (or simply inner product), i.e.,

$$\langle a, b \rangle_\Omega := \int_\Omega ab \, d\Omega \quad \text{and} \quad \langle \mathbf{c}, \mathbf{d} \rangle_\Omega := \int_\Omega \mathbf{c} \cdot \mathbf{d} \, d\Omega,$$

if  $a, b$  are scalar fields and  $\mathbf{c}, \mathbf{d}$  are vector fields in  $\Omega$ .

**Complement 2.1** For an instruction of evaluating the integration numerically, see script [quadrature.py] [www.mathischeap.com/contents/LIBRARY/ptc/quadrature](http://www.mathischeap.com/contents/LIBRARY/ptc/quadrature).

The space  $H^1(\Omega)$ , a subspace of the  $L^2(\Omega)$ , is defined as

$$H^1(\Omega) := \{\psi \mid \psi \in L^2(\Omega), \nabla \psi \in [L^2(\Omega)]^n\},$$

where we have used  $n$  to denote the dimensions of the space. If  $\Omega$  is a sub-domain of  $\mathbb{R}^2$  ( $n = 2$ ), we know that the curl of a scalar field gives a vector field, and we distinguish it from the rotation operator which works on a vector and gives a scalar. Therefore, we define  $H(\text{curl}; \Omega)$  and  $H(\text{rot}; \Omega)$  in  $\mathbb{R}^2$  as

$$H(\text{curl}; \Omega) := \left\{ \phi \mid \phi \in L^2(\Omega), \nabla \times \phi = \begin{bmatrix} \frac{\partial \phi}{\partial y} & -\frac{\partial \phi}{\partial x} \end{bmatrix}^\top \in [L^2(\Omega)]^2 \right\},$$

$$H(\text{rot}; \Omega) := \left\{ \mathbf{v} \mid \mathbf{v} = [v_1 \ v_2]^\top \in [L^2(\Omega)]^2, \nabla \times \mathbf{v} = \frac{\partial v_2}{\partial x} - \frac{\partial v_1}{\partial y} \in L^2(\Omega) \right\}.$$

Note that we have used  $\nabla \times$  to denote both rotation and curl operators and we can identify which operator it is by checking the type (scalar or vector) of the object it is working on. In  $\mathbb{R}^3$ , curl and rotation operators are equivalent. Thus

$$H(\text{curl}; \Omega) = H(\text{rot}; \Omega) := \left\{ \mathbf{v} \mid \mathbf{v} \in [L^2(\Omega)]^3, \nabla \times \mathbf{v} \in [L^2(\Omega)]^3 \right\}.$$

Analogously, we can define the space  $H(\text{div}; \Omega)$ :

$$H(\text{div}; \Omega) := \left\{ \mathbf{u} \mid \mathbf{u} \in [L^2(\Omega)]^n, \nabla \cdot \mathbf{u} \in L^2(\Omega) \right\}.$$

The trace operator, denoted by  $T$ , restricts a function defined in  $\Omega$  to its boundary. In  $\mathbb{R}^3$ , we consider the following trace spaces. The  $H^{1/2}(\partial\Omega)$  space, a subspace of  $L^2(\partial\Omega)$ , is the range

<sup>2</sup>More generally,  $C$  can be an arbitrary scalar field such that  $\nabla C = \mathbf{0}$ .

(or image) of the trace operator on  $H^1(\Omega)$ , i.e.,

$$H^{1/2}(\partial\Omega) := \left\{ \widehat{\psi} \mid \exists \psi \in H^1(\Omega), \widehat{\psi} = T\psi \text{ on } \partial\Omega \right\}.$$

Its dual space  $H^{-1/2}(\partial\Omega)$  is defined as the range of the trace operator on  $H(\text{div}; \Omega)$ ,

$$H^{-1/2}(\partial\Omega) := \{ \widehat{u} \mid \exists \mathbf{u} \in H(\text{div}; \Omega), \widehat{u} = T\mathbf{u} = \mathbf{u} \cdot \mathbf{n} \text{ on } \partial\Omega \}.$$

For  $H(\text{curl}; \Omega)$ , we consider two trace operators,  $T_{\parallel}$  and  $T_{\perp}$  and the corresponding traces spaces are defined as

$$\begin{aligned} TH_{\parallel}(\partial\Omega) &:= \{ \widehat{\boldsymbol{\omega}} \mid \exists \boldsymbol{\omega} \in H(\text{curl}; \Omega), \widehat{\boldsymbol{\omega}} = T_{\parallel}\boldsymbol{\omega} = \mathbf{n} \times (\boldsymbol{\omega} \times \mathbf{n}) \text{ on } \partial\Omega \}, \\ TH_{\perp}(\partial\Omega) &:= \{ \widehat{\boldsymbol{\omega}} \mid \exists \boldsymbol{\omega} \in H(\text{curl}; \Omega), \widehat{\boldsymbol{\omega}} = T_{\perp}\boldsymbol{\omega} = \boldsymbol{\omega} \times \mathbf{n} \text{ on } \partial\Omega \}. \end{aligned}$$

The vector  $\mathbf{n} \times (\boldsymbol{\omega} \times \mathbf{n})$  is the component of  $\boldsymbol{\omega}$  parallel to the tangent plane of  $\partial\Omega$ , and we have

$$(2.2) \quad \boldsymbol{\omega} = \mathbf{n} \times (\boldsymbol{\omega} \times \mathbf{n}) + (\boldsymbol{\omega} \cdot \mathbf{n}) \mathbf{n}$$

with  $(\boldsymbol{\omega} \cdot \mathbf{n}) \mathbf{n}$  being the component of  $\boldsymbol{\omega}$  perpendicular to the tangent plane. The vector  $\boldsymbol{\omega} \times \mathbf{n}$  is also parallel to the tangent plane and is perpendicular to  $\boldsymbol{\omega}$  and  $\mathbf{n} \times (\boldsymbol{\omega} \times \mathbf{n})$  because the cross product of two vectors is perpendicular to either vector, i.e.,

$$(2.3) \quad (\mathbf{a} \times \mathbf{b}) \perp \mathbf{a} \quad \text{and} \quad (\mathbf{a} \times \mathbf{b}) \perp \mathbf{b}.$$

See Fig. 2.1 for an illustration of the decomposition of  $\boldsymbol{\omega} \in H(\text{curl}; \Omega)$  on the domain boundary. Trace spaces  $TH_{\parallel}(\partial\Omega)$  and  $TH_{\perp}(\partial\Omega)$  are also a pair of dual spaces. And for more information on the trace spaces, we refer to, for example, [122, 123].

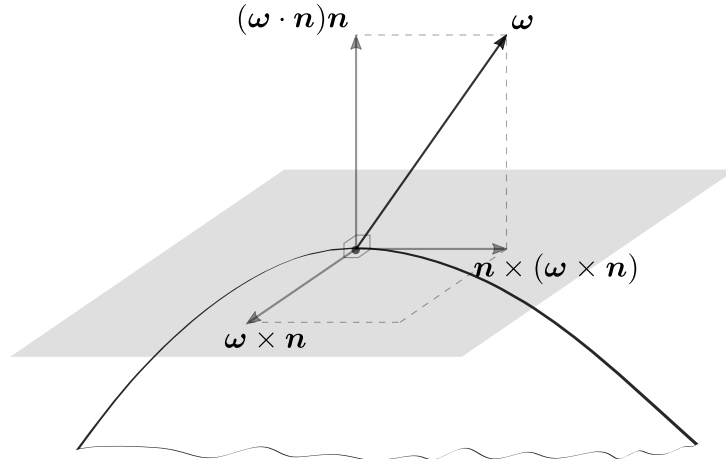


FIGURE 2.1: An illustration of the decomposition of  $\boldsymbol{\omega} \in H(\text{curl}; \Omega)$  on the domain boundary.

### 2.2.2 The de Rham complex

The de Rham complex formally is a concept in differential geometry [31, 83, 124–127]. It is a sequence of differential  $k$ -form spaces,  $\Lambda^k(\Omega)$ , unidirectionally connected by the exterior derivative,  $d$ . A generalized form of the de Rham complex is given as

$$(2.4) \quad 0 \hookrightarrow \Lambda^0(\Omega) \xrightarrow{d} \Lambda^1(\Omega) \xrightarrow{d} \dots \xrightarrow{d} \Lambda^n(\Omega) \longrightarrow 0.$$

In terms of Sobolev spaces, the de Rham complex has different forms in different dimensions:

- In  $\mathbb{R}^1$ , we have

$$\begin{aligned} 0 &\hookrightarrow H^1(\Omega) \xrightarrow{\nabla} L^2(\Omega) \rightarrow 0, \\ 0 &\hookrightarrow H(\operatorname{div}; \Omega) \xrightarrow{\nabla \cdot} L^2(\Omega) \rightarrow 0, \end{aligned}$$

where in this case  $H^1(\Omega) = H(\operatorname{div}; \Omega)$  and both the gradient and the divergence operators refer to the derivative operator,  $d$ . Note that, see (2.4), we have also used the notation  $d$  to express the exterior derivative for differential forms.

- In  $\mathbb{R}^2$ , we have

$$\begin{aligned} 0 &\hookrightarrow H^1(\Omega) \xrightarrow{\nabla} H(\operatorname{rot}; \Omega) \xrightarrow{\nabla \times} L^2(\Omega) \rightarrow 0, \\ 0 &\hookrightarrow H(\operatorname{curl}; \Omega) \xrightarrow{\nabla \times} H(\operatorname{div}; \Omega) \xrightarrow{\nabla \cdot} L^2(\Omega) \rightarrow 0. \end{aligned}$$

- In  $\mathbb{R}^3$ , the de Rham complex is of the form,

$$(2.5) \quad 0 \hookrightarrow H^1(\Omega) \xrightarrow{\nabla} H(\operatorname{curl}; \Omega) \xrightarrow{\nabla \times} H(\operatorname{div}; \Omega) \xrightarrow{\nabla \cdot} L^2(\Omega) \rightarrow 0.$$

Such a complex implies that the range of an operator is a subspace of the next space, to be more exact, is a subspace of the null space of the next space with respect to the next operator. Recall the fact that  $\nabla \times \nabla(\cdot) \equiv \mathbf{0}$  and  $\nabla \cdot \nabla \times (\cdot) \equiv 0$ . A visualization of the de Rham complex in  $\mathbb{R}^3$ , (2.5), is shown in Fig. 2.2.

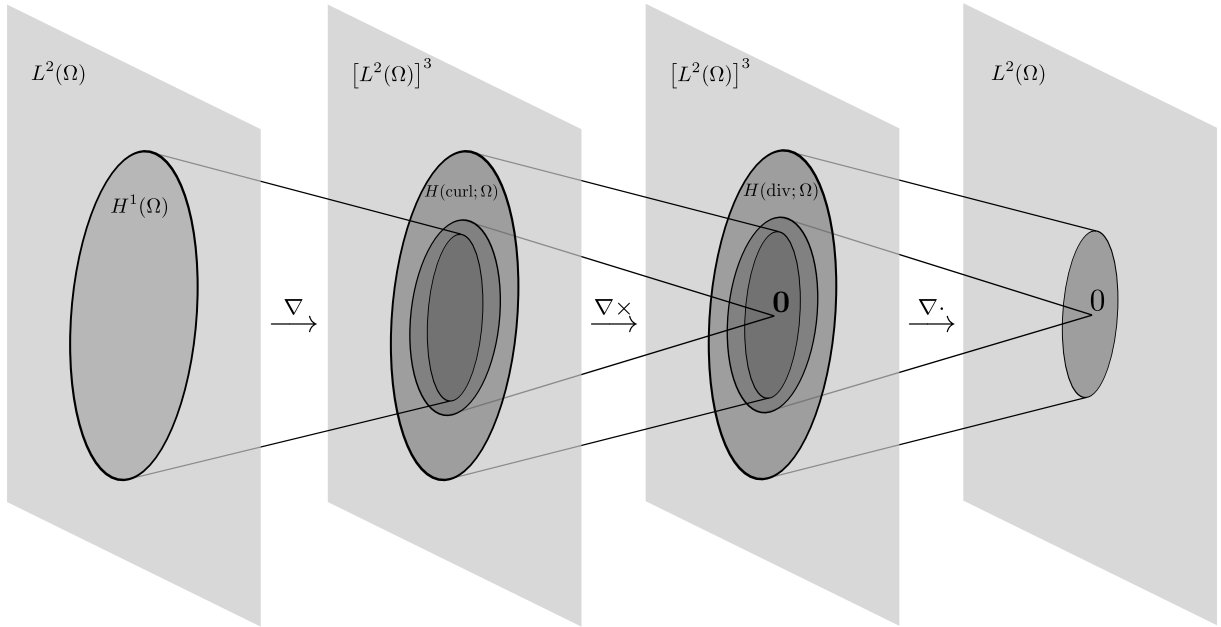


FIGURE 2.2: A visualization of the de Rham complex of Sobolev spaces in  $\mathbb{R}^3$ .

We call the first order differential operators,  $\nabla$ ,  $\nabla \times$  and  $\nabla \cdot$ , the *primal differential operators* or simply *primal operators* and call the corresponding complexes, for example, (2.5), the *primal de Rham complexes*. The primal operators are topological operators and the MSEM will preserve the topological structure of them at the discrete level, which will be explained later in this chapter.

### 2.2.3 Double de Rham complex

To introduce the double de Rham complex, we restrict ourselves to  $\mathbb{R}^3$  as an example.

In terms of the  $L^2$ -inner product, integration by parts with respect to the primal divergence operator induces an adjoint operator of it. The adjoint operator is defined as

$$(2.6) \quad \widetilde{\nabla} : L^2(\Omega) \rightarrow H(\operatorname{div}; \Omega),$$

such that

$$(2.7) \quad \left\langle \mathbf{v}, \widetilde{\nabla} \varphi \right\rangle_{\Omega} = - \langle \nabla \cdot \mathbf{v}, \varphi \rangle_{\Omega} + \int_{\partial\Omega} \varphi (\mathbf{v} \cdot \mathbf{n}) \, d\Gamma \quad \forall \mathbf{v} \in H(\operatorname{div}; \Omega).$$

This adjoint operator,  $\widetilde{\nabla}$ , is called the *dual gradient operator*.

As for the primal curl operator, integration by parts in terms of the inner product induces an adjoint operator defined as

$$(2.8) \quad \widetilde{\nabla} \times : H(\operatorname{div}; \Omega) \rightarrow H(\operatorname{curl}; \Omega),$$

such that

$$(2.9) \quad \left\langle \boldsymbol{\omega}, \widetilde{\nabla} \times \mathbf{u} \right\rangle_{\Omega} = \langle \nabla \times \boldsymbol{\omega}, \mathbf{u} \rangle_{\Omega} - \int_{\partial\Omega} \boldsymbol{\omega} \cdot (\mathbf{u} \times \mathbf{n}) \, d\Gamma \quad \forall \boldsymbol{\omega} \in H(\operatorname{curl}; \Omega).$$

Note that on the boundary  $\boldsymbol{\omega} \cdot (\mathbf{u} \times \mathbf{n}) = (T_{\parallel} \boldsymbol{\omega}) \cdot (\mathbf{u} \times \mathbf{n})$  as the perpendicular component of  $\boldsymbol{\omega}$ ,  $(\boldsymbol{\omega} \cdot \mathbf{n}) \mathbf{n}$ , does not contribute to this dot product, i.e.,  $(\boldsymbol{\omega} \cdot \mathbf{n}) \mathbf{n} \perp \mathbf{u} \times \mathbf{n}$ , see (2.2) and (2.3). And we call this adjoint operator,  $\widetilde{\nabla} \times$ , the *dual curl operator*.

Analogously, integration by parts with respect to the primal gradient operator induces an adjoint operator defined as

$$(2.10) \quad \widetilde{\nabla} \cdot : H(\operatorname{curl}; \Omega) \rightarrow H^1(\Omega),$$

such that

$$(2.11) \quad \left\langle \psi, \widetilde{\nabla} \cdot \boldsymbol{\omega} \right\rangle_{\Omega} = - \langle \nabla \psi, \boldsymbol{\omega} \rangle_{\Omega} + \int_{\partial\Omega} \psi (\boldsymbol{\omega} \cdot \mathbf{n}) \, d\Gamma \quad \forall \psi \in H^1(\Omega).$$

We call this adjoint operator,  $\widetilde{\nabla} \cdot$ , the *dual divergence operator*.

**Remark 2.1** *Performing the dual operators can be done by computing the corresponding primal operators employing integration by parts. It will also need the assistance of the additional trace variable for the boundary integral. For example, in (2.7), since  $\varphi \in L^2(\Omega)$ , it does not admit a trace operator. Thus*

$$\varphi|_{\partial\Omega} \in H^{1/2}(\partial\Omega)$$

*has to be an additional boundary variable provided for the calculation of the dual gradient operator. Similarly, in (2.9) and (2.11),  $\mathbf{u} \in H(\operatorname{div}; \Omega)$  and  $\boldsymbol{\omega} \in H(\operatorname{curl}; \Omega)$  do not admit trace operators  $T_{\perp}$  and  $T$  respectively. That is to say, boundary variables*

$$\mathbf{u} \times \mathbf{n} \in TH_{\perp}(\partial\Omega) \quad \text{and} \quad \boldsymbol{\omega} \cdot \mathbf{n} \in H^{-1/2}(\partial\Omega)$$

need to be provided for computing the dual curl and divergence operators, respectively. Therefore, more precise expressions, instead of (2.6), (2.8) and (2.10), for the dual operators are

$$\begin{aligned}\widetilde{\nabla} &: L^2(\Omega) \times H^{1/2}(\partial\Omega) \rightarrow H(\operatorname{div}; \Omega), \\ \widetilde{\nabla} \times &: H(\operatorname{div}; \Omega) \times TH_{\perp}(\partial\Omega) \rightarrow H(\operatorname{curl}; \Omega), \\ \widetilde{\nabla} \cdot &: H(\operatorname{curl}; \Omega) \times H^{-1/2}(\partial\Omega) \rightarrow H^1(\Omega).\end{aligned}$$

As they do not impact the introduction of the MSEM, we temporarily leave them as shown in (2.6), (2.8) and (2.10) for neatness. This is also the case when the MSEM was initially proposed.

With these dual operators, we can extend the primal de Rham complex, (2.5), to a double de Rham complex as shown in Fig. 2.3. The  $L^2$ -inner product is metric-dependent and we will see later in this chapter that in the MSEM we perform the dual operator through integration by parts in terms of the  $L^2$ -inner product.

$$\begin{array}{ccccccccc} \mathbb{R} & \hookrightarrow & H^1(\Omega) & \xrightarrow{\nabla} & H(\operatorname{curl}; \Omega) & \xrightarrow{\nabla \times} & H(\operatorname{div}; \Omega) & \xrightarrow{\nabla \cdot} & L^2(\Omega) & \longrightarrow & 0 \\ & & \updownarrow & & \updownarrow & & \updownarrow & & \updownarrow & & \\ 0 & \longleftarrow & H^1(\Omega) & \xleftarrow{\widetilde{\nabla} \cdot} & H(\operatorname{curl}; \Omega) & \xleftarrow{\widetilde{\nabla} \times} & H(\operatorname{div}; \Omega) & \xleftarrow{\widetilde{\nabla}} & L^2(\Omega) & \longleftarrow & \mathbb{R} \end{array}$$

FIGURE 2.3: The double de Rham complex in  $\mathbb{R}^3$ . The upper branch is the *primal de Rham complex* and the lower branch is called the *dual de Rham complex*. Note that we have omitted the trace spaces in the dual de Rham complex, see Remark 2.1.

## 2.2.4 de Rham structure of the Poisson problem

In this section, we use the double de Rham complex to analyze the Poisson equations (2.1). If we select  $\varphi \in H^1(\Omega)$ , we will have  $\mathbf{u} = k\nabla\varphi \in H(\operatorname{curl}; \Omega)$  with the gradient operator being a primal operator. This implies that the operator working on  $\mathbf{u}$  in (2.1b) must be a dual divergence operator, see Fig. 2.3. Thus, original equations (2.1a) and (2.1b) can be expressed as a weak form<sup>3</sup>: For  $(\mathbf{u}, \varphi) \in H(\operatorname{curl}; \Omega) \times H^1(\Omega)$ ,

$$(2.12a) \quad \mathbf{u} = k\nabla\varphi \quad \text{in } \Omega,$$

$$(2.12b) \quad \widetilde{\nabla} \cdot \mathbf{u} = -f \quad \text{in } \Omega.$$

Alternatively, we can take the divergence operator as a primal operator and take the gradient operator as a dual one. As a result, the original equations (2.1a) and (2.1b) can be expressed as the following weak form:  $(\mathbf{u}, \varphi) \in H(\operatorname{div}; \Omega) \times L^2(\Omega)$

$$(2.13a) \quad \mathbf{u} = k\widetilde{\nabla}\varphi \quad \text{in } \Omega,$$

$$(2.13b) \quad \nabla \cdot \mathbf{u} = -f \quad \text{in } \Omega.$$

These interpretations reflect two particular structures, see Fig. 2.4, in the double de Rham complex.

For the MSEM, we prefer to use the right de Rham structure of Fig. 2.4 which takes the gradient operator as a dual operator and takes the divergence operator as the primal one. This

<sup>3</sup>It is a weak form in the sense that we have restrict  $\mathbf{u}$  and  $\varphi$  to particular spaces that do not contain all scalars or vectors.

$$\begin{array}{ccc}
\longrightarrow H^1(\Omega) & \xrightarrow{\nabla} & H(\text{curl}; \Omega) \longrightarrow \\
\uparrow & & \downarrow k \\
\longleftarrow H^1(\Omega) & \xleftarrow{\widetilde{\nabla}} & H(\text{curl}; \Omega) \longleftarrow
\end{array}
\qquad
\begin{array}{ccc}
\longrightarrow H(\text{div}; \Omega) & \xrightarrow{\nabla \cdot} & L^2(\Omega) \longrightarrow \\
\uparrow k & & \downarrow \\
\longleftarrow H(\text{div}; \Omega) & \xleftarrow{\widetilde{\nabla}} & L^2(\Omega) \longleftarrow
\end{array}$$

FIGURE 2.4: Two de Rham structures of the Poisson problem. The interpretation (2.12) reflects the left structure while the interpretation (2.13) reflects the right structure.

is because that including the material parameter will need the help of metric terms (which will be explained later in this chapter). Thus in this way the topological structure of the divergence relation which stands for a fundamental conservation law can be preserved at the discrete level by the MSEM.

It does not mean that the left de Rham structure in Fig. 2.4 is not applicable for the MSEM. We can still use it. However, the resulting discretization is less preferable because we will setup a topological discretization for the constitutive relation but introduce metric terms for the discretization of the topological relation.

Using the right de Rham structure of Fig. 2.4, we now can rewrite the Poisson problem (2.1) in a weak form with Sobolev spaces as follows: Given  $f \in L^2(\Omega)$ , boundary conditions  $\widehat{\varphi} \in H^{1/2}(\Gamma_\varphi)$  and  $\widehat{u} \in H^{-1/2}(\Gamma_\varphi)$ , find  $(\mathbf{u}, \varphi) \in H(\text{div}; \Omega) \times L^2(\Omega)$  such that

$$\begin{aligned}
(2.14a) \quad & \mathbf{u} = k \widetilde{\nabla} \varphi && \text{in } \Omega, \\
(2.14b) \quad & \nabla \cdot \mathbf{u} = -f && \text{in } \Omega, \\
(2.14c) \quad & \varphi = \widehat{\varphi} && \text{on } \Gamma_\varphi, \\
(2.14d) \quad & \mathbf{u} \cdot \mathbf{n} = \widehat{u} && \text{on } \Gamma_{\mathbf{u}}.
\end{aligned}$$

### 2.2.5 A weak formulation of the Poisson problem

If we test (2.14a) with test function  $\mathbf{v} \in H_0(\text{div}; \Omega)$ ,

$$H_0(\text{div}; \Omega) := \{\mathbf{v} \mid \mathbf{v} \in H(\text{div}; \Omega), \mathbf{v} \cdot \mathbf{n} = 0 \text{ on } \Gamma_{\mathbf{u}}\},$$

and test (2.14b) with test function  $\phi \in L^2(\Omega)$ , applying integration by parts (2.7) to the dual gradient term, we can obtain the following weak formulation of the problem (2.14): Given  $f \in L^2(\Omega)$ , boundary conditions  $\widehat{\varphi} \in H^{1/2}(\Gamma_\varphi)$  and  $\widehat{u} \in H^{-1/2}(\Gamma_{\mathbf{u}})$ , seek  $(\mathbf{u}, \varphi) \in H_{\widehat{u}}(\text{div}; \Omega) \times L^2(\Omega)$  such that

$$(2.15a) \quad \langle \mathbf{v}, k^{-1} \mathbf{u} \rangle_\Omega + \langle \nabla \cdot \mathbf{v}, \varphi \rangle_\Omega = \int_{\Gamma_\varphi} \widehat{\varphi} (\mathbf{v} \cdot \mathbf{n}) \quad \forall \mathbf{v} \in H_0(\text{div}; \Omega),$$

$$(2.15b) \quad \langle \phi, \nabla \cdot \mathbf{u} \rangle_\Omega = - \langle \phi, f \rangle_\Omega \quad \forall \phi \in L^2(\Omega),$$

where the space  $H_{\widehat{u}}(\text{div}; \Omega)$  is defined as

$$H_{\widehat{u}}(\text{div}; \Omega) := \{\mathbf{u} \mid \mathbf{u} \in H(\text{div}; \Omega), \mathbf{u} \cdot \mathbf{n} = \widehat{u} \text{ on } \Gamma_{\mathbf{u}}\}.$$

For an alternative approach to obtain this weak formulation based on a constrained minimization problem, we refer to, for example, [31, 117].

### 2.3 Mimetic polynomials

So far, all analysis is conducted at the continuous level. In this section, we introduce the discrete or finite dimensional function spaces to be used for the discretization with the MSEM.

The MSEM, as mentioned before, aims to preserve the de Rham structure at the discrete level. In order to achieve so, it must use discrete function spaces which are able to form a *discrete de Rham complex*. If there is a set of discrete functions spaces,

$$\{G(\Omega), C(\Omega), D(\Omega), S(\Omega)\},$$

such that

$$(2.16) \quad \begin{array}{ccc} G(\Omega) & \subset & H^1(\Omega) \\ \downarrow \nabla & & \downarrow \nabla \\ C(\Omega) & \subset & H(\text{curl}; \Omega) \\ \downarrow \nabla \times & & \downarrow \nabla \times \\ D(\Omega) & \subset & H(\text{div}; \Omega) \\ \downarrow \nabla \cdot & & \downarrow \nabla \cdot \\ S(\Omega) & \subset & L^2(\Omega) \end{array},$$

we say that they constitute a discrete de Rham complex, see Fig. 2.2, and call these spaces a set of *mimetic* or *structure-preserving* spaces.

There are multiple particular sets of mimetic spaces. One well-known choice is to employ  $G(\Omega) = \text{CG}_N$ ,  $C(\Omega) = \text{NED}_N^1$ ,  $D(\Omega) = \text{RT}_N$ , and  $S(\Omega) = \text{DG}_{N-1}$ , i.e.,

$$\begin{array}{ccc} \text{CG}_N & \subset & H^1(\Omega) \\ \downarrow \nabla & & \downarrow \nabla \\ \text{NED}_N^1 & \subset & H(\text{curl}; \Omega) \\ \downarrow \nabla \times & & \downarrow \nabla \times \\ \text{RT}_N & \subset & H(\text{div}; \Omega) \\ \downarrow \nabla \cdot & & \downarrow \nabla \cdot \\ \text{DG}_{N-1} & \subset & L^2(\Omega) \end{array},$$

where  $\text{CG}_N$  are the continuous Galerkin spaces of degree  $N$ ,  $\text{NED}_N^1$  are the Nédélec  $H(\text{curl})$ -conforming spaces of the first kind of degree  $N$ , see [55],  $\text{RT}_N$  are the Raviart-Thomas spaces of degree  $N$ , see [54, 55], and  $\text{DG}_{N-1}$  are the discontinuous Galerkin spaces of degree  $(N - 1)$ . Another possible set of mimetic spaces employing B-splines is used in the works by Hiemstra et al. [114], Buffa et al. [128], Ratnani and Sonnendrücker [129] and Zhang et al. [130].

A third choice is the mimetic spaces which will be used in this chapter. In this section, we will introduce the construction of these mimetic spaces. We will first introduce the construction of them in the reference domain. Afterwards, transforming them from the reference domain to general, orthogonal or curvilinear, domains will be explained. In the reference domain, they are spaces of polynomials and thus are called the *mimetic polynomial spaces*. While in a general domain, depending on the mapping, it is not guaranteed that they are spaces of polynomials. And from now on, the general term, mimetic spaces, refer to these particular mimetic spaces in

this chapter.

### 2.3.1 Lagrange polynomials and edge polynomials

In  $\mathbb{R}^1$ , the mimetic polynomials consist of the well-known *Lagrange polynomials* and the *edge polynomials* [32]. For completeness, we start with a brief introduction of the Lagrange polynomials. Let a set of nodes,  $\{\xi_0, \xi_1, \dots, \xi_N\}$ , partition the 1D reference domain,  $I_{\text{ref}} = [-1, 1]$ ,

$$-1 = \xi_0 < \xi_1 < \dots < \xi_N = 1.$$

And throughout the thesis, we will use the Legendre-Gauss-Lobatto (LGL) nodes. The Lagrange polynomials,

$$l^i(\xi) := \prod_{j=0, j \neq i}^N \frac{\xi - \xi_j}{\xi_i - \xi_j}, \quad i \in \{0, 1, \dots, N\},$$

are polynomials of degree  $N$  which satisfy a nodal Kronecker delta property expressed as

$$(2.17) \quad l^i(\xi_j) = \delta_j^i = \begin{cases} 1 & \text{if } i = j \\ 0 & \text{else} \end{cases}.$$

The edge polynomials of degree  $(N - 1)$ ,  $e^i(\xi)$ , are linear combinations of the derivatives of the Lagrange polynomials, i.e.,

$$(2.18) \quad e^i(\xi) := \sum_{j=i}^N \frac{dl^j(\xi)}{d\xi} = - \sum_{j=0}^{i-1} \frac{dl^j(\xi)}{d\xi}, \quad i \in \{1, 2, \dots, N\},$$

which satisfy an integral Kronecker delta property expressed as

$$(2.19) \quad \int_{\xi_{j-1}}^{\xi_j} e^i(\xi) d\xi = \delta_j^i.$$

Examples of Lagrange polynomials and edge polynomials are shown in Fig. 2.5.

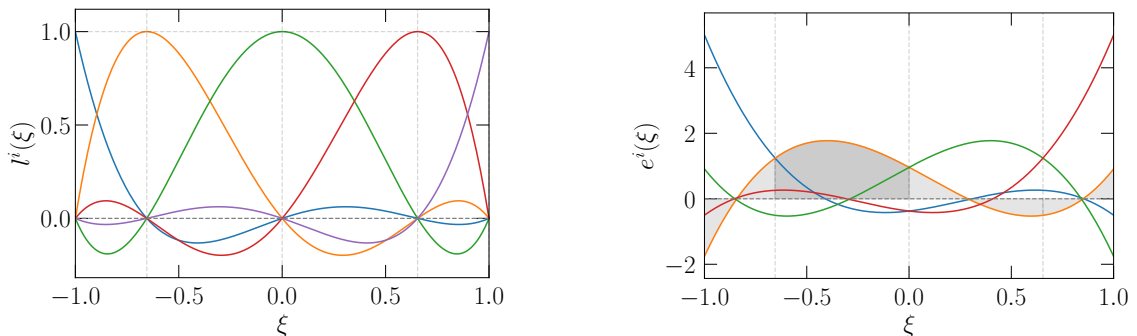


FIGURE 2.5: Lagrange polynomials (left) and edge polynomials (right) derived from a partition of degree 4,  $-1 = \xi_0 < \xi_1 < \dots < \xi_4 = 1$ . The vertical gray dashed lines indicate the internal nodes,  $\xi_1, \xi_2, \xi_3$ . The nodal Kronecker delta property (2.17) is obvious. The integral Kronecker delta property (2.19) can be seen, for example, from the edge polynomial  $e_2(\xi)$  (orange solid line). Direct calculations will reveal that  $\int_{\xi_1}^{\xi_2} e^2(\xi) d\xi = 1$  and  $\int_{\xi_{j-1}}^{\xi_j} e^2(\xi) d\xi = 0$ ,  $j \in \{1, 3, 4\}$ .

**Complement 2.2** For a Python implementation of Lagrange polynomials and edge polynomials in the 1D reference domain, see the script  
`[Lagrange_and_edge_polynomials.py]`  
[www.mathischeap.com/contents/LIBRARY/ptc/Lagrange\\_and\\_edge\\_polynomials](http://www.mathischeap.com/contents/LIBRARY/ptc/Lagrange_and_edge_polynomials).

In  $I_{\text{ref}}$ , the Lagrange polynomials span a discrete polynomial space denoted by  $\text{LP}_N(I_{\text{ref}})$ , i.e.,

$$\text{LP}_N(I_{\text{ref}}) := \text{span}(\{l^0(\xi), l^1(\xi), \dots, l^N(\xi)\}),$$

and the edge polynomials span a discrete polynomial space denoted by  $\text{EP}_{N-1}(I_{\text{ref}})$ , i.e.,

$$\text{EP}_{N-1}(I_{\text{ref}}) := \text{span}(\{e^1(\xi), e^2(\xi), \dots, e^N(\xi)\}).$$

※ Polynomials in spaces  $\text{LP}_N(I_{\text{ref}})$  and  $\text{EP}_{N-1}(I_{\text{ref}})$  are of the following forms.

- A polynomial  $p^h \in \text{LP}_N(I_{\text{ref}})$  is of the form

$$p^h(\xi) = \sum_{i=0}^N \mathbf{p}_i l^i(\xi),$$

where  $\mathbf{p}_i \in \mathbb{R}$  are the expansion coefficients (degrees of freedom) of the polynomial. And, from the nodal Kronecker delta property (2.17), it is easy to find

$$(2.20) \quad p^h(\xi_i) \stackrel{(2.17)}{=} \mathbf{p}_i.$$

- A polynomial  $q^h \in \text{EP}_{N-1}(I_{\text{ref}})$  is of the form

$$q^h(\xi) = \sum_{i=1}^N \mathbf{q}_i e^i(\xi),$$

where  $\mathbf{q}_i \in \mathbb{R}$  are the expansion coefficients of the polynomial. From the integral Kronecker delta property (2.19), we know

$$(2.21) \quad \int_{\xi_{i-1}}^{\xi_i} q^h(\xi) d\xi \stackrel{(2.19)}{=} \mathbf{q}_i.$$

If, for  $p^h \in \text{LP}_N(I_{\text{ref}})$  and  $q^h \in \text{EP}_{N-1}(I_{\text{ref}})$ , the following relation holds,

$$(2.22) \quad q^h(\xi) = \frac{dp^h(\xi)}{d\xi},$$

we integrate  $q^h$  over line segments  $[\xi_{i-1}, \xi_i]$ , and, using the first fundamental theorem of calculus and relations (2.20) and (2.21), we can find that

$$(2.23) \quad \mathbf{q}_i = \mathbf{p}_i - \mathbf{p}_{i-1}, \quad i \in \{1, 2, \dots, N\}.$$

This suggests a discrete counterpart for the derivative operator. Let us collect the expansion coefficients of  $p^h$  and  $q^h$ , and put them in column vectors denoted by  $\underline{p}$  and  $\underline{q}$ , i.e.,

$$\underline{p} := [\mathbf{p}_0 \quad \mathbf{p}_1 \quad \cdots \quad \mathbf{p}_N]^\top \quad \text{and} \quad \underline{q} := [\mathbf{q}_1 \quad \mathbf{q}_2 \quad \cdots \quad \mathbf{p}_N]^\top.$$

Note that this convention, using underlined symbols to denote column vectors of expansion coefficients, will be used throughout the chapter. From (2.23), we can find that there is a linear operator, the so-called *incidence matrix*,  $\mathbf{E}$ , such that

$$(2.24) \quad \underline{q} = \mathbf{E}\underline{p},$$

where the incidence matrix  $\mathbf{E}$  is an  $N$  by  $(N+1)$  sparse (only if  $N > 1$ ) matrix with two nonzero entries,  $\mathbf{E}|_{i,i-1} = -1$  and  $\mathbf{E}|_{i,i} = 1$ , per row. For example, if  $N = 4$ , we have

$$\mathbf{E} = \begin{bmatrix} -1 & 1 & 0 & 0 & 0 \\ 0 & -1 & 1 & 0 & 0 \\ 0 & 0 & -1 & 1 & 0 \\ 0 & 0 & 0 & -1 & 1 \end{bmatrix}.$$

The incidence matrix  $\mathbf{E}$  is a topological matrix; it contains  $-1$ ,  $+1$  and  $0$  and only depends on the topology of the grid. For example, if we use a different set of nodes,  $-1 = \xi_0 < \xi'_1 < \xi'_2 < \cdots < \xi'_{N-1} < \xi_N = 1$ , although the resulting Lagrange polynomials and edge polynomials will be different, the relation (2.23) remains the same. This means the incidence matrix  $\mathbf{E}$  will be the same. Also note that (2.23) is exact, which implies that  $\mathbf{E}$  is an exact discrete counterpart of the derivative operator, see (2.22) and (2.24). In other words, it is a derivative operator applied to the degrees of freedom.

Application of the derivative operator to a polynomial in  $\text{LP}_N(I_{\text{ref}})$  thus can be done easily through applying the linear operator,  $\mathbf{E}$ , to the column vector of expansion coefficients. The resulting column vector contains the expansion coefficients of the resulting polynomial in  $\text{EP}_{N-1}(I_{\text{ref}})$ . Since such a process is valid for all polynomials in  $\text{LP}_N(I_{\text{ref}})$ , i.e.,

$$(2.25) \quad dp^h \in \text{EP}_{N-1}(I_{\text{ref}}) \quad \forall p^h \in \text{LP}_N(I_{\text{ref}}),$$

we can conclude that the mimetic polynomial spaces  $\text{LP}_N(I_{\text{ref}})$  and  $\text{EP}_{N-1}(I_{\text{ref}})$  form a 1D discrete de Rham complex,

$$\mathbb{R} \hookrightarrow \text{LP}_N(I_{\text{ref}}) \xrightarrow{d} \text{EP}_{N-1}(I_{\text{ref}}) \rightarrow 0,$$

where the derivative operator,  $d$ , has an exact discrete counterpart, the incidence matrix  $\mathbf{E}$ . Note that the subscripts,  $N$  and  $N-1$ , indicate the degrees of the polynomials in the spaces.

### 2.3.2 Mimetic polynomials in the reference domain of $\mathbb{R}^3$

In  $\mathbb{R}^3$  equipped with an orthogonal coordinate system  $(\xi, \eta, \varsigma)$ , consider the reference domain  $\Omega_{\text{ref}} = [-1, 1]^3$ . Let three sets of nodes,

$$\{\xi_0, \xi_1, \cdots, \xi_{N_\xi}\}, \{\eta_0, \eta_1, \cdots, \eta_{N_\eta}\} \quad \text{and} \quad \{\varsigma_0, \varsigma_1, \cdots, \varsigma_{N_\varsigma}\},$$

partition the interval  $[-1, 1]$ , i.e.,  $-1 = \xi_0 < \xi_1 < \cdots < \xi_{N_\xi} = 1$ ,  $-1 = \eta_0 < \eta_1 < \cdots < \eta_{N_\eta} = 1$  and  $-1 = \varsigma_0 < \varsigma_1 < \cdots < \varsigma_{N_\varsigma} = 1$ . Without the loss of generality, we use  $N_\xi = N_\eta = N_\varsigma = N$ . Based on these sets of nodes, we can construct the following 1D Lagrange polynomials and edge

polynomials along three axes,

$$(2.26a) \quad \{l^0(\xi), l^1(\xi), \dots, l^N(\xi)\},$$

$$(2.26b) \quad \{l^0(\eta), l^1(\eta), \dots, l^N(\eta)\},$$

$$(2.26c) \quad \{l^0(\varsigma), l^1(\varsigma), \dots, l^N(\varsigma)\},$$

$$(2.26d) \quad \{e^1(\xi), e^2(\xi), \dots, e^N(\xi)\},$$

$$(2.26e) \quad \{e^1(\eta), e^2(\eta), \dots, e^N(\eta)\},$$

$$(2.26f) \quad \{e^1(\varsigma), e^2(\varsigma), \dots, e^N(\varsigma)\}.$$

**Node polynomials** If we perform the tensor product to Lagrange polynomials (2.26a), (2.26b) and (2.26c), we can obtain a set of polynomials,

$$(2.27) \quad \left\{ \text{lll}^{i,j,k}(\xi, \eta, \varsigma) \mid i, j, k \in \{0, 1, \dots, N\} \right\},$$

where  $\text{lll}^{i,j,k}(\xi, \eta, \varsigma) := l^i(\xi)l^j(\eta)l^k(\varsigma)$ . If we use the following notation to denote points

$$(2.28) \quad P_{l,m,n} = (\xi_l, \eta_m, \varsigma_n), \quad l, m, n \in \{0, 1, \dots, N\},$$

from (2.17), it is easy to see that these polynomials satisfy the nodal Kronecker delta property,

$$(2.29) \quad \text{lll}^{i,j,k}(P_{l,m,n}) = l^i(\xi_l)l^j(\eta_m)l^k(\varsigma_n) = \delta_{l,m,n}^{i,j,k} = \begin{cases} 1 & \text{if } i = l, j = m, k = n \\ 0 & \text{else} \end{cases}.$$

We call these polynomials the *basis node polynomials*. The discrete space of node polynomials,  $\text{NP}_N(\Omega_{\text{ref}})$ , is the space spanned by these basis node polynomials, i.e.,

$$(2.30) \quad \text{NP}_N(\Omega_{\text{ref}}) := \text{span} \left( \left\{ \text{lll}^{i,j,k}(\xi, \eta, \varsigma) \mid i, j, k \in \{0, 1, \dots, N\} \right\} \right).$$

**Edge polynomials** Similarly, using the 1D Lagrange polynomials and edge polynomials, we can construct following polynomials,

$$(2.31a) \quad \left\{ \text{ell}^{i,j,k}(\xi, \eta, \varsigma) \mid i \in \{1, 2, \dots, N\}, j, k \in \{0, 1, \dots, N\} \right\},$$

$$(2.31b) \quad \left\{ \text{lel}^{i,j,k}(\xi, \eta, \varsigma) \mid j \in \{1, 2, \dots, N\}, i, k \in \{0, 1, \dots, N\} \right\},$$

$$(2.31c) \quad \left\{ \text{lle}^{i,j,k}(\xi, \eta, \varsigma) \mid k \in \{1, 2, \dots, N\}, i, j \in \{0, 1, \dots, N\} \right\},$$

where we have used notations

$$\text{ell}^{i,j,k}(\xi, \eta, \varsigma) := e^i(\xi)l^j(\eta)l^k(\varsigma),$$

$$\text{lel}^{i,j,k}(\xi, \eta, \varsigma) := l^i(\xi)e^j(\eta)l^k(\varsigma),$$

$$\text{lle}^{i,j,k}(\xi, \eta, \varsigma) := l^i(\xi)l^j(\eta)e^k(\varsigma).$$

We introduce following notations for the edges,

$$(2.33a) \quad E_{l,m,n}^\xi := ([\xi_{l-1}, \xi_l], \eta_m, \varsigma_n),$$

$$(2.33b) \quad E_{l,m,n}^\eta := (\xi_l, [\eta_{m-1}, \eta_m], \varsigma_n),$$

$$(2.33c) \quad E_{l,m,n}^\varsigma := (\xi_l, \eta_m, [\varsigma_{n-1}, \varsigma_n]).$$

For example,  $E_{l,m,n}^\xi$  is the edge connecting the points  $P_{l-1,m,n}$  and  $P_{l,m,n}$  and  $E_{l,m,n}^\eta$  is the edge connecting the points  $P_{l,m-1,n}$  and  $P_{l,m,n}$ . With the Kronecker delta properties (2.17) and (2.19), we can find that polynomials in (2.31) satisfy line integral Kronecker delta properties expressed as

$$(2.34a) \quad \int_{E_{l,m,n}^\xi} \text{ell}^{i,j,k}(\xi, \eta, \varsigma) dr = \int_{\xi_{l-1}}^{\xi_l} e^i(\xi) d\xi l^j(\eta_m) l^k(\varsigma_n) = \delta_{l,m,n}^{i,j,k},$$

$$(2.34b) \quad \int_{E_{l,m,n}^\eta} \text{lel}^{i,j,k}(\xi, \eta, \varsigma) dr = l^i(\xi_l) \int_{\eta_{m-1}}^{\eta_m} e^j(\eta) d\eta l^k(\varsigma_n) = \delta_{l,m,n}^{i,j,k},$$

$$(2.34c) \quad \int_{E_{l,m,n}^\varsigma} \text{lle}^{i,j,k}(\xi, \eta, \varsigma) dr = l^i(\xi_l) l^j(\eta_m) \int_{\varsigma_{n-1}}^{\varsigma_n} e^k(\varsigma) d\varsigma = \delta_{l,m,n}^{i,j,k}.$$

We call these polynomials the *basis edge polynomials*. The discrete space of edge polynomials<sup>4</sup> (note the difference from the 1D edge polynomials, see (2.18)), denoted by  $\text{EP}_{N-1}(\Omega_{\text{ref}})$ , is the space spanned by these basis edge polynomials, i.e.,

$$(2.35) \quad \begin{aligned} \text{EP}_{N-1}(\Omega_{\text{ref}}) &:= \text{span} \left( \left\{ \text{ell}^{i,j,k}(\xi, \eta, \varsigma) \mid i \in \{1, 2, \dots, N\}, j, k \in \{0, 1, \dots, N\} \right\} \right) \\ &\times \text{span} \left( \left\{ \text{lel}^{i,j,k}(\xi, \eta, \varsigma) \mid j \in \{1, 2, \dots, N\}, i, k \in \{0, 1, \dots, N\} \right\} \right) \\ &\times \text{span} \left( \left\{ \text{lle}^{i,j,k}(\xi, \eta, \varsigma) \mid k \in \{1, 2, \dots, N\}, i, j \in \{0, 1, \dots, N\} \right\} \right). \end{aligned}$$

**Face polynomials** It is also possible to construct polynomials,

$$(2.36a) \quad \left\{ \text{lee}^{i,j,k}(\xi, \eta, \varsigma) \mid i \in \{0, 1, \dots, N\}, j, k \in \{1, 2, \dots, N\} \right\},$$

$$(2.36b) \quad \left\{ \text{ele}^{i,j,k}(\xi, \eta, \varsigma) \mid j \in \{0, 1, \dots, N\}, i, k \in \{1, 2, \dots, N\} \right\},$$

$$(2.36c) \quad \left\{ \text{eel}^{i,j,k}(\xi, \eta, \varsigma) \mid k \in \{0, 1, \dots, N\}, i, j \in \{1, 2, \dots, N\} \right\},$$

using the 1D Lagrange polynomials and edge polynomials. And we have used notations

$$\text{lee}^{i,j,k}(\xi, \eta, \varsigma) := l^i(\xi) e^j(\eta) e^k(\varsigma),$$

$$\text{ele}^{i,j,k}(\xi, \eta, \varsigma) := e^i(\xi) l^j(\eta) e^k(\varsigma),$$

$$\text{eel}^{i,j,k}(\xi, \eta, \varsigma) := e^i(\xi) e^j(\eta) l^k(\varsigma).$$

<sup>4</sup>We call them polynomials despite they are actually vectors of polynomials.

We denote the following faces by

$$(2.38a) \quad F_{l,m,n}^\xi := (\xi_l, [\eta_{m-1}, \eta_m], [\varsigma_{n-1}, \varsigma_n]),$$

$$(2.38b) \quad F_{l,m,n}^\eta := ([\xi_{l-1}, \xi_l], \eta_m, [\varsigma_{n-1}, \varsigma_n]),$$

$$(2.38c) \quad F_{l,m,n}^\varsigma := ([\xi_{l-1}, \xi_l], [\eta_{m-1}, \eta_m], \varsigma_n),$$

For example,  $F_{l,m,n}^\xi$  is the face whose four corners are points  $P_{l,m-1,n-1}$ ,  $P_{l,m,n-1}$ ,  $P_{l,m,n}$  and  $P_{l,m,n-1}$ . Analogously, with the Kronecker delta properties for the 1D polynomials, (2.17) and (2.19), we can easily verify that these polynomials satisfy the following surface integral Kronecker delta properties,

$$(2.39a) \quad \int_{F_{l,m,n}^\xi} \text{lee}^{i,j,k}(\xi, \eta, \varsigma) d\Gamma = l^i(\xi_l) \int_{\eta_{m-1}}^{\eta_m} e^j(\eta) d\eta \int_{\varsigma_{n-1}}^{\varsigma_n} e^k(\varsigma) d\varsigma = \delta_{l,m,n}^{i,j,k},$$

$$(2.39b) \quad \int_{F_{l,m,n}^\eta} \text{ele}^{i,j,k}(\xi, \eta, \varsigma) d\Gamma = \int_{\xi_{l-1}}^{\xi_l} e^i(\xi) d\xi l^j(\eta_m) \int_{\varsigma_{n-1}}^{\varsigma_n} e^k(\varsigma) d\varsigma = \delta_{l,m,n}^{i,j,k},$$

$$(2.39c) \quad \int_{F_{l,m,n}^\varsigma} \text{eel}^{i,j,k}(\xi, \eta, \varsigma) d\Gamma = \int_{\xi_{l-1}}^{\xi_l} e^i(\xi) d\xi \int_{\eta_{m-1}}^{\eta_m} e^j(\eta) d\eta l^k(\varsigma_n) = \delta_{l,m,n}^{i,j,k}.$$

We call these polynomials the *basis face polynomials*. The discrete space of face polynomials<sup>5</sup>, denoted by  $\text{FP}_{N-1}(\Omega_{\text{ref}})$ , is the space spanned by these basis face polynomials, i.e.,

$$(2.40) \quad \begin{aligned} \text{FP}_{N-1}(\Omega_{\text{ref}}) &:= \text{span} \left( \left\{ \text{lee}^{i,j,k}(\xi, \eta, \varsigma) \mid i \in \{0, 1, \dots, N\}, j, k \in \{1, 2, \dots, N\} \right\} \right) \\ &\times \text{span} \left( \left\{ \text{ele}^{i,j,k}(\xi, \eta, \varsigma) \mid j \in \{0, 1, \dots, N\}, i, k \in \{1, 2, \dots, N\} \right\} \right) \\ &\times \text{span} \left( \left\{ \text{eel}^{i,j,k}(\xi, \eta, \varsigma) \mid k \in \{0, 1, \dots, N\}, i, j \in \{1, 2, \dots, N\} \right\} \right). \end{aligned}$$

**Volume polynomials** If we perform the tensor product to the 1D edge polynomials in (2.26d), (2.26e) and (2.26f), we can get the following polynomials,

$$(2.41) \quad \left\{ \text{eee}^{i,j,k}(\xi, \eta, \varsigma) \mid i, j, k \in \{1, 2, \dots, N\} \right\},$$

where  $\text{eee}^{i,j,k}(\xi, \eta, \varsigma) := e^i(\xi)e^j(\eta)e^k(\varsigma)$ . The following notation is used to denote the volumes

$$(2.42) \quad V_{l,m,n} := ([\xi_{l-1}, \xi_l], [\eta_{m-1}, \eta_m], [\varsigma_{n-1}, \varsigma_n]),$$

See Complement 2.3 for an illustration of these volumes. Derived from the integral Kronecker property of the 1D edge polynomials, (2.19), these polynomials satisfy a volume integral Kronecker delta property expressed as

$$(2.43) \quad \int_{V_{l,m,n}} \text{eee}^{i,j,k}(\xi, \eta, \varsigma) dV = \int_{\xi_{l-1}}^{\xi_l} e^i(\xi) d\xi \int_{\eta_{m-1}}^{\eta_m} e^j(\eta) d\eta \int_{\varsigma_{n-1}}^{\varsigma_n} e^k(\varsigma) d\varsigma = \delta_{l,m,n}^{i,j,k}.$$

<sup>5</sup>We call them polynomials despite they are actually vectors of polynomials.

We call them the *basis volume polynomials*. They span a discrete space of volume polynomials, denoted by  $VP_{N-1}(\Omega_{\text{ref}})$ ,

$$(2.44) \quad VP_{N-1}(\Omega_{\text{ref}}) := \text{span} \left( \left\{ \text{eee}^{i,j,k}(\xi, \eta, \varsigma) \mid i, j, k \in \{1, 2, \dots, N\} \right\} \right).$$

**Complement 2.3** For an illustration of the distribution of the geometric objects to which the polynomials are related through Kronecker properties (2.29), (2.34), (2.39) and (2.43), see document [geometries\_and\_distribution.pdf]  
[www.mathischeap.com/contents/LIBRARY/ptc/geometries\\_and\\_distribution](http://www.mathischeap.com/contents/LIBRARY/ptc/geometries_and_distribution).

※ Discrete polynomials in spaces  $NP_N(\Omega_{\text{ref}})$ ,  $EP_{N-1}(\Omega_{\text{ref}})$ ,  $FP_{N-1}(\Omega_{\text{ref}})$  and  $VP_{N-1}(\Omega_{\text{ref}})$  are of the following forms.

- A node polynomial  $\psi^h \in NP_N(\Omega_{\text{ref}})$  is of the form

$$\psi^h(\xi, \eta, \varsigma) = \sum_{i=0}^N \sum_{j=0}^N \sum_{k=0}^N \Psi_{i,j,k} \text{lll}^{i,j,k}(\xi, \eta, \varsigma),$$

where  $\Psi_{i,j,k} \in \mathbb{R}$  are the expansion coefficients of the node polynomial. And we know, from the Kronecker delta property (2.29), that

$$(2.45) \quad \psi^h(P_{l,m,n}) = \sum_{i=0}^N \sum_{j=0}^N \sum_{k=0}^N \Psi_{i,j,k} \text{lll}^{i,j,k}(\xi_l, \eta_m, \varsigma_n) \stackrel{(2.29)}{=} \Psi_{l,m,n}.$$

- An edge polynomial  $\omega^h \in EP_{N-1}(\Omega_{\text{ref}})$  is of the form

$$\omega^h(\xi, \eta, \varsigma) = \begin{bmatrix} \sum_{i=1}^N \sum_{j=0}^N \sum_{k=0}^N w_{i,j,k}^{\xi} \text{ell}^{i,j,k}(\xi, \eta, \varsigma) \\ \sum_{i=0}^N \sum_{j=1}^N \sum_{k=0}^N w_{i,j,k}^{\eta} \text{lel}^{i,j,k}(\xi, \eta, \varsigma) \\ \sum_{i=0}^N \sum_{j=0}^N \sum_{k=1}^N w_{i,j,k}^{\varsigma} \text{lle}^{i,j,k}(\xi, \eta, \varsigma) \end{bmatrix},$$

where  $w_{i,j,k}^{\xi}, w_{i,j,k}^{\eta}, w_{i,j,k}^{\varsigma} \in \mathbb{R}$  are the expansion coefficients of the edge polynomial. From Kronecker delta properties (2.34), we know that

$$(2.46a) \quad \int_{E_{l,m,n}^{\xi}} \omega^h \cdot d\mathbf{r} = \int_{E_{l,m,n}^{\xi}} \sum_{i=1}^N \sum_{j=0}^N \sum_{k=0}^N w_{i,j,k}^{\xi} \text{ell}^{i,j,k}(\xi, \eta, \varsigma) d\mathbf{r} \stackrel{(2.34a)}{=} w_{l,m,n}^{\xi},$$

$$(2.46b) \quad \int_{E_{l,m,n}^{\eta}} \omega^h \cdot d\mathbf{r} = \int_{E_{l,m,n}^{\eta}} \sum_{i=0}^N \sum_{j=1}^N \sum_{k=0}^N w_{i,j,k}^{\eta} \text{lel}^{i,j,k}(\xi, \eta, \varsigma) d\mathbf{r} \stackrel{(2.34b)}{=} w_{l,m,n}^{\eta},$$

$$(2.46c) \quad \int_{E_{l,m,n}^{\varsigma}} \omega^h \cdot d\mathbf{r} = \int_{E_{l,m,n}^{\varsigma}} \sum_{i=0}^N \sum_{j=0}^N \sum_{k=1}^N w_{i,j,k}^{\varsigma} \text{lle}^{i,j,k}(\xi, \eta, \varsigma) d\mathbf{r} \stackrel{(2.34c)}{=} w_{l,m,n}^{\varsigma}.$$

- A face polynomial  $\mathbf{u}^h \in \text{FP}_{N-1}(\Omega_{\text{ref}})$  is of the form

$$\mathbf{u}^h(\xi, \eta, \varsigma) = \begin{bmatrix} \sum_{i=0}^N \sum_{j=1}^N \sum_{k=1}^N u_{i,j,k}^\xi \text{lee}^{i,j,k}(\xi, \eta, \varsigma) \\ \sum_{i=1}^N \sum_{j=0}^N \sum_{k=1}^N u_{i,j,k}^\eta \text{ele}^{i,j,k}(\xi, \eta, \varsigma) \\ \sum_{i=1}^N \sum_{j=1}^N \sum_{k=0}^N u_{i,j,k}^\varsigma \text{eel}^{i,j,k}(\xi, \eta, \varsigma) \end{bmatrix},$$

where  $u_{i,j,k}^\xi, u_{i,j,k}^\eta, u_{i,j,k}^\varsigma \in \mathbb{R}$  are the expansion coefficients of the face polynomial. And we know, from Kronecker delta properties (2.39), that

$$(2.47a) \quad \int_{F_{l,m,n}^\xi} \mathbf{u}^h \cdot \mathbf{n} \, d\Gamma = \int_{F_{l,m,n}^\xi} \sum_{i=0}^N \sum_{j=1}^N \sum_{k=1}^N u_{i,j,k}^\xi \text{lee}^{i,j,k}(\xi, \eta, \varsigma) d\Gamma \stackrel{(2.39a)}{=} u_{l,m,n}^\xi,$$

$$(2.47b) \quad \int_{F_{l,m,n}^\eta} \mathbf{u}^h \cdot \mathbf{n} \, d\Gamma = \int_{F_{l,m,n}^\eta} \sum_{i=1}^N \sum_{j=0}^N \sum_{k=1}^N u_{i,j,k}^\eta \text{ele}^{i,j,k}(\xi, \eta, \varsigma) d\Gamma \stackrel{(2.39b)}{=} u_{l,m,n}^\eta,$$

$$(2.47c) \quad \int_{F_{l,m,n}^\varsigma} \mathbf{u}^h \cdot \mathbf{n} \, d\Gamma = \int_{F_{l,m,n}^\varsigma} \sum_{i=1}^N \sum_{j=1}^N \sum_{k=0}^N u_{i,j,k}^\varsigma \text{eel}^{i,j,k}(\xi, \eta, \varsigma) d\Gamma \stackrel{(2.39c)}{=} u_{l,m,n}^\varsigma.$$

- A volume polynomial  $\mathbf{f}^h \in \text{VP}_{N-1}(\Omega_{\text{ref}})$  is of the form

$$\mathbf{f}^h(\xi, \eta, \varsigma) = \sum_{i=1}^N \sum_{j=1}^N \sum_{k=1}^N f_{i,j,k} \text{eee}^{i,j,k}(\xi, \eta, \varsigma),$$

where  $f_{i,j,k} \in \mathbb{R}$  are the expansion coefficients of the volume polynomial. And we know, from the Kronecker delta property (2.43), that

$$(2.48) \quad \int_{V_{l,m,n}} \mathbf{f}^h \, dV = \int_{V_{l,m,n}} \sum_{i=1}^N \sum_{j=1}^N \sum_{k=1}^N f_{i,j,k} \text{eee}^{i,j,k}(\xi, \eta, \varsigma) dV \stackrel{(2.43)}{=} f_{l,m,n}.$$

**Incidence matrix**  $E_{(\nabla)}$  Given  $\psi^h \in \text{NP}_N(\Omega)$  and  $\boldsymbol{\omega}^h \in \text{EP}_{N-1}(\Omega_{\text{ref}})$ , if

$$(2.49) \quad \boldsymbol{\omega}^h = \nabla \psi^h,$$

we integrate  $\boldsymbol{\omega}^h$  along edges  $E_{i,k,j}^\xi$ ,  $E_{i,k,j}^\eta$  and  $E_{i,k,j}^\varsigma$ , and with the gradient theorem for line integrals and properties (2.45) and (2.46), we can easily find that

$$(2.50a) \quad w_{i,j,k}^\xi = \Psi_{i,j,k} - \Psi_{i-1,j,k}, \quad i \in \{1, 2, \dots, N\}, \quad j, k \in \{0, 1, \dots, N\},$$

$$(2.50b) \quad w_{i,j,k}^\eta = \Psi_{i,j,k} - \Psi_{i,j-1,k}, \quad j \in \{1, 2, \dots, N\}, \quad i, k \in \{0, 1, \dots, N\},$$

$$(2.50c) \quad w_{i,j,k}^\varsigma = \Psi_{i,j,k} - \Psi_{i,j,k-1}, \quad k \in \{1, 2, \dots, N\}, \quad i, j \in \{0, 1, \dots, N\}.$$

We now number the expansion coefficients of  $\psi^h$  as

$$(2.51) \quad \Psi_{i+1+j(N+1)+k(N+1)^2} = \Psi_{i,j,k},$$

and number the expansion coefficients of  $\omega^h$  as

$$(2.52a) \quad \mathbf{w}_{i+jN+kN(N+1)} = \mathbf{w}_{i,j,k}^\xi,$$

$$(2.52b) \quad \mathbf{w}_{i+1+(j-1)(N+1)+kN(N+1)+N(N+1)^2} = \mathbf{w}_{i,j,k}^\eta,$$

$$(2.52c) \quad \mathbf{w}_{i+1+j(N+1)+(k-1)(N+1)^2+2N(N+1)^2} = \mathbf{w}_{i,j,k}^\zeta.$$

We call a numbering a *local numbering* if it relates an indexing to a sequence of increasing positive integers,  $\{1, 2, \dots\}$ . With the local numberings (2.51) and (2.52), we can summarize (2.50) into an algebraic relation expressed as

$$(2.53) \quad \underline{\omega} = \mathbf{E}_{(\nabla)} \underline{\psi},$$

where  $\underline{\psi} := [\Psi_1 \ \Psi_2 \ \dots \ \Psi_{(N+1)^3}]^\top$ ,  $\underline{\omega} := [\mathbf{w}_1 \ \mathbf{w}_2 \ \dots \ \mathbf{w}_{3N(N+1)^2}]^\top$  and the linear operator  $\mathbf{E}_{(\nabla)}$  is the incidence matrix of the gradient operator at the discrete level, see (2.49). For example, if  $N = 1$ , the incidence matrix  $\mathbf{E}_{(\nabla)}$  is given as

$$(2.54) \quad \mathbf{E}_{(\nabla)} = \begin{bmatrix} -1 & 1 & 0 & 0 & 0 & 0 & 0 & 0 \\ 0 & 0 & -1 & 1 & 0 & 0 & 0 & 0 \\ 0 & 0 & 0 & 0 & -1 & 1 & 0 & 0 \\ 0 & 0 & 0 & 0 & 0 & 0 & -1 & 1 \\ -1 & 0 & 1 & 0 & 0 & 0 & 0 & 0 \\ 0 & -1 & 0 & 1 & 0 & 0 & 0 & 0 \\ 0 & 0 & 0 & 0 & -1 & 0 & 1 & 0 \\ 0 & 0 & 0 & 0 & 0 & -1 & 0 & 1 \\ -1 & 0 & 0 & 0 & 1 & 0 & 0 & 0 \\ 0 & -1 & 0 & 0 & 0 & 1 & 0 & 0 \\ 0 & 0 & -1 & 0 & 0 & 0 & 1 & 0 \\ 0 & 0 & 0 & -1 & 0 & 0 & 0 & 1 \end{bmatrix}.$$

**Incidence matrix  $\mathbf{E}_{(\nabla \times)}$**  Similarly, given  $\omega^h \in \text{EP}_{N-1}(\Omega_{\text{ref}})$ ,  $\mathbf{u}^h \in \text{FP}_{N-1}(\Omega_{\text{ref}})$  and

$$(2.55) \quad \mathbf{u}^h = \nabla \times \omega^h,$$

if we integrate  $\mathbf{u}^h$  over faces  $F_{i,k,j}^\xi$ ,  $F_{i,k,j}^\eta$  and  $F_{i,k,j}^\zeta$ , with the Stokes' integral theorem and properties (2.46) and (2.47), we will obtain

$$(2.56a) \quad \mathbf{u}_{i,j,k}^\xi = +\mathbf{w}_{i,j,k-1}^\eta - \mathbf{w}_{i,j,k}^\eta - \mathbf{w}_{i,j-1,k}^\zeta + \mathbf{w}_{i,j,k}^\zeta, \quad i \in \{0, 1, \dots, N\}, \quad j, k \in \{1, 2, \dots, N\},$$

$$(2.56b) \quad \mathbf{u}_{i,j,k}^\eta = -\mathbf{w}_{i,j,k-1}^\xi + \mathbf{w}_{i,j,k}^\xi + \mathbf{w}_{i-1,j,k}^\zeta - \mathbf{w}_{i,j,k}^\zeta, \quad j \in \{0, 1, \dots, N\}, \quad i, k \in \{1, 2, \dots, N\},$$

$$(2.56c) \quad \mathbf{u}_{i,j,k}^\zeta = +\mathbf{w}_{i,j-1,k}^\xi - \mathbf{w}_{i,j,k}^\xi - \mathbf{w}_{i-1,j,k}^\eta + \mathbf{w}_{i,j,k}^\eta, \quad k \in \{0, 1, \dots, N\}, \quad i, j \in \{1, 2, \dots, N\}.$$

If we apply a local numbering to the expansion coefficients of  $\mathbf{u}^h$ , for example,

$$(2.57a) \quad \mathbf{u}_{i+1+(j-1)(N+1)+(k-1)N(N+1)} = \mathbf{u}_{i,j,k}^\xi,$$

$$(2.57b) \quad \mathbf{u}_{i+jN+(k-1)N(N+1)+N^2(N+1)} = \mathbf{u}_{i,j,k}^\eta,$$

$$(2.57c) \quad \mathbf{u}_{i+(j-1)N+kN^2+2N^2(N+1)} = \mathbf{u}_{i,j,k}^\sigma,$$

the relations in (2.56) can be summarized as a linear algebra equality,

$$(2.58) \quad \underline{\mathbf{u}} = \mathbf{E}_{(\nabla \times)} \underline{\boldsymbol{\omega}},$$

where  $\underline{\mathbf{u}} := [\mathbf{u}_1 \ \mathbf{u}_2 \ \cdots \ \mathbf{u}_{3N^2(N+1)}]^\top$  is the column vector of the expansion coefficients of  $\mathbf{u}^h$  and  $\mathbf{E}_{(\nabla \times)}$  is the incidence matrix for the curl operator at the discrete level, see (2.55). For example, if  $N = 1$ , the incidence matrix  $\mathbf{E}_{(\nabla \times)}$  is given as

$$(2.59) \quad \mathbf{E}_{(\nabla \times)} = \begin{bmatrix} 0 & 0 & 0 & 0 & 1 & 0 & -1 & 0 & -1 & 0 & 1 & 0 \\ 0 & 0 & 0 & 0 & 0 & 1 & 0 & -1 & 0 & -1 & 0 & 1 \\ -1 & 0 & 1 & 0 & 0 & 0 & 0 & 0 & 1 & -1 & 0 & 0 \\ 0 & -1 & 0 & 1 & 0 & 0 & 0 & 0 & 0 & 0 & 1 & -1 \\ 1 & -1 & 0 & 0 & -1 & 1 & 0 & 0 & 0 & 0 & 0 & 0 \\ 0 & 0 & 1 & -1 & 0 & 0 & -1 & 1 & 0 & 0 & 0 & 0 \end{bmatrix}.$$

**Incidence matrix  $\mathbf{E}_{(\nabla \cdot)}$**  For  $\mathbf{u}^h \in \text{FP}_{N-1}(\Omega_{\text{ref}})$  and  $f^h \in \text{VP}_{N-1}(\Omega_{\text{ref}})$ , if

$$(2.60) \quad f^h = \nabla \cdot \mathbf{u}^h,$$

we integrate  $f^h$  over volumes  $V_{i,j,k}$  and, with Gauss' integral theorem and properties (2.47) and (2.48), we will find that

$$(2.61) \quad \mathbf{f}_{i,j,k} = \mathbf{u}_{i,j,k}^\xi - \mathbf{u}_{i-1,j,k}^\xi + \mathbf{u}_{i,j,k}^\eta - \mathbf{u}_{i,j-1,k}^\eta + \mathbf{u}_{i,j,k}^\zeta - \mathbf{u}_{i,j,k-1}^\zeta, \quad i, j, k \in \{1, 2, \dots, N\}.$$

If we use the local numbering

$$(2.62) \quad \mathbf{f}_{i+(j-1)N+(k-1)N^2} = \mathbf{f}_{i,j,k},$$

and introduce the column vector  $\underline{\mathbf{f}} := [\mathbf{f}_1 \ \mathbf{f}_2 \ \cdots \ \mathbf{f}_{N^3}]^\top$ , we can summarize (2.61) into an algebra relation,

$$(2.63) \quad \underline{\mathbf{f}} = \mathbf{E}_{(\nabla \cdot)} \underline{\mathbf{u}},$$

where the incidence matrix  $\mathbf{E}_{(\nabla \cdot)}$  is the incidence matrix for the divergence operator at the discrete level, see (2.60). For example, if  $N = 1$ , the incidence matrix  $\mathbf{E}_{(\nabla \cdot)}$  is a 1 by 6 matrix given as

$$(2.64) \quad \mathbf{E}_{(\nabla \cdot)} = \begin{bmatrix} -1 & 1 & -1 & 1 & -1 & 1 \end{bmatrix}.$$

**Complement 2.4** For an illustration of local numberings (2.51), (2.52), (2.57) and (2.62), see document [local\_numberings.pdf]  
[www.mathischeap.com/contents/LIBRARY/ptc/local\\_numberings](http://www.mathischeap.com/contents/LIBRARY/ptc/local_numberings).

**Complement 2.5** For a Python implementation of the basis *node*, *edge*, *face* and *volume* polynomials under aforementioned local numberings, see script [mimetic\_basis\_polynomials.py]  
[www.mathischeap.com/contents/LIBRARY/ptc/mimetic\\_basis\\_polynomials](http://www.mathischeap.com/contents/LIBRARY/ptc/mimetic_basis_polynomials).

**Complement 2.6** For a Python implementation and more examples of incidence matrices,  $E_{(\nabla)}$ ,  $E_{(\nabla \times)}$  and  $E_{(\nabla \cdot)}$ , see script [incidence\_matrices.py]  
[www.mathischeap.com/contents/LIBRARY/ptc/incidence\\_matrices](http://www.mathischeap.com/contents/LIBRARY/ptc/incidence_matrices).

Note that the local numberings are not unique; different local numberings will lead to different incidence matrices (with row and column permutations) while the relations (2.53), (2.58) and (2.63) still hold.

Like the incidence matrix  $E$  in  $\mathbb{R}^1$ , see (2.24), the incidence matrices  $E_{(\nabla)}$ ,  $E_{(\nabla \times)}$  and  $E_{(\nabla \cdot)}$  are also sparse (except for  $E_{(\nabla \cdot)}$  at  $N = 1$ , see (2.64)) and topological in the sense that they only contain nonzero entries of  $-1$  and  $1$  and only depend on  $N$  and the local numberings regardless of the distribution of the nodes on which the mimetic polynomials are based. And since (2.50), (2.56) and (2.61) are exact, incidence matrices  $E_{(\nabla)}$ ,  $E_{(\nabla \times)}$  and  $E_{(\nabla \cdot)}$  are exact discrete counterparts of gradient, curl and divergence operators applied to the expansion coefficients. Following the same analysis as for (2.25), we can easily conclude that

$$\begin{aligned} \nabla \psi^h &\in EP_{N-1}(\Omega_{\text{ref}}) & \forall \psi^h &\in NP_N(\Omega_{\text{ref}}), \\ \nabla \times \boldsymbol{\omega}^h &\in FP_{N-1}(\Omega_{\text{ref}}) & \forall \boldsymbol{\omega}^h &\in EP_{N-1}(\Omega_{\text{ref}}), \\ \nabla \cdot \mathbf{u}^h &\in VP_{N-1}(\Omega_{\text{ref}}) & \forall \mathbf{u}^h &\in FP_{N-1}(\Omega_{\text{ref}}). \end{aligned}$$

Thus we know the mimetic polynomial spaces

$$NP_N(\Omega_{\text{ref}}), \quad EP_{N-1}(\Omega_{\text{ref}}), \quad FP_{N-1}(\Omega_{\text{ref}}) \quad \text{and} \quad VP_{N-1}(\Omega_{\text{ref}})$$

form a discrete de Rham complex,

$$\begin{array}{ccc} NP_N(\Omega_{\text{ref}}) & \subset & H^1(\Omega_{\text{ref}}) \\ \downarrow \nabla & & \downarrow \nabla \\ EP_{N-1}(\Omega_{\text{ref}}) & \subset & H(\text{curl}; \Omega_{\text{ref}}) \\ \downarrow \nabla \times & & \downarrow \nabla \times \\ FP_{N-1}(\Omega_{\text{ref}}) & \subset & H(\text{div}; \Omega_{\text{ref}}) \\ \downarrow \nabla \cdot & & \downarrow \nabla \cdot \\ VP_{N-1}(\Omega_{\text{ref}}) & \subset & L^2(\Omega_{\text{ref}}) \end{array},$$

where the primal operators,  $\nabla$ ,  $\nabla \times$  and  $\nabla \cdot$ , have exact discrete counterparts, the incidence matrices,  $E_{(\nabla)}$ ,  $E_{(\nabla \times)}$  and  $E_{(\nabla \cdot)}$ . And because of the fact that  $\nabla \times \nabla(\cdot) \equiv \mathbf{0}$  and  $\nabla \cdot \nabla \times (\cdot) \equiv 0$ , we must have

$$E_{(\nabla \times)} E_{(\nabla)} \equiv \mathbf{0} \quad \text{and} \quad E_{(\nabla \cdot)} E_{(\nabla \times)} \equiv \mathbf{0}.$$

One can easily check this using examples of incidence matrices in (2.54), (2.59) and (2.64), see

Complement 2.6. The subscripts,  $N$  and  $N - 1$ , refer to the overall degrees of the polynomials in the spaces, and we call  $\text{NP}_N(\Omega_{\text{ref}})$ ,  $\text{EP}_{N-1}(\Omega_{\text{ref}})$ ,  $\text{FP}_{N-1}(\Omega_{\text{ref}})$  and  $\text{VP}_{N-1}(\Omega_{\text{ref}})$  a set of mimetic polynomial spaces of degree  $N$ .

### 2.3.3 Mimetic basis functions in general domains of $\mathbb{R}^3$

So far we have introduced the construction of mimetic polynomials only in the reference element. In this section, we will introduce how to construct mimetic basis functions in a general domain.

We consider a general domain  $\Omega$  which can be obtained by transforming the reference domain  $\Omega_{\text{ref}}$  using a  $C^1$  diffeomorphism mapping  $\Phi$  (both  $\Phi$  and its inverse mapping,  $\Phi^{-1} : \Omega \rightarrow \Omega_{\text{ref}}$  are  $C^1$  continuous),

$$(2.65) \quad \Phi : \Omega_{\text{ref}} \rightarrow \Omega.$$

The mimetic basis functions in  $\Omega$  can be constructed by transforming the mimetic polynomials in the reference domain.

**Remark 2.2** *The indexing and the local numbering of the mimetic polynomials in the reference domain will be inherited by the mimetic basis functions in  $\Omega$ .*

**Coordinate transformation** Let the general domain be equipped with a coordinate system  $(x, y, z)$ . A general form of the mapping (2.65) is expressed as

$$\mathbf{x} = (x, y, z) = \Phi(\xi, \eta, \varsigma) = (\Phi_x(\xi, \eta, \varsigma), \Phi_y(\xi, \eta, \varsigma), \Phi_z(\xi, \eta, \varsigma)).$$

Its Jacobian matrix  $\mathcal{J}$  is given as

$$\mathcal{J} := \begin{bmatrix} \frac{\partial x}{\partial \xi} & \frac{\partial x}{\partial \eta} & \frac{\partial x}{\partial \varsigma} \\ \frac{\partial y}{\partial \xi} & \frac{\partial y}{\partial \eta} & \frac{\partial y}{\partial \varsigma} \\ \frac{\partial z}{\partial \xi} & \frac{\partial z}{\partial \eta} & \frac{\partial z}{\partial \varsigma} \end{bmatrix} = [\mathbf{x}_\xi \quad \mathbf{x}_\eta \quad \mathbf{x}_\varsigma],$$

where we have introduced column vectors  $\mathbf{x}_\xi$ ,  $\mathbf{x}_\eta$  and  $\mathbf{x}_\varsigma$ . The Jacobian of the mapping is the determinant of the Jacobian matrix,  $\det(\mathcal{J})$ , and the metric matrix is

$$\mathcal{G} = \begin{bmatrix} g_{1,1} & g_{1,2} & g_{1,3} \\ g_{2,1} & g_{2,2} & g_{2,3} \\ g_{3,1} & g_{3,2} & g_{3,3} \end{bmatrix} = \mathcal{J}^\top \mathcal{J},$$

where, to be more explicit,

$$g_{i,j} = \sum_{l=1}^3 \mathcal{J}|_{l,i} \mathcal{J}|_{l,j}, \quad i, j \in \{1, 2, 3\}.$$

The metric matrix is symmetric and positive definite. The metric of the mapping is defined as the determinant of the metric matrix and is equal to the square of the Jacobian,

$$g = \det(\mathcal{G}) = [\det(\mathcal{J})]^2.$$

And from the fact  $\Phi^{-1} \circ \Phi : \Omega \rightarrow \Omega$ , we know that  $\mathcal{J}^{-1}\mathcal{J} = \mathcal{I}$ , where  $\mathcal{I}$  is the identity matrix. The inverse Jacobian matrix, the Jacobian matrix of the inverse mapping,  $\Phi^{-1} : \Omega \rightarrow \Omega_{\text{ref}}$ , is

$$\mathcal{J}^{-1} := \begin{bmatrix} \frac{\partial \xi}{\partial x} & \frac{\partial \xi}{\partial y} & \frac{\partial \xi}{\partial z} \\ \frac{\partial \eta}{\partial x} & \frac{\partial \eta}{\partial y} & \frac{\partial \eta}{\partial z} \\ \frac{\partial \varsigma}{\partial x} & \frac{\partial \varsigma}{\partial y} & \frac{\partial \varsigma}{\partial z} \end{bmatrix} = \begin{bmatrix} \nabla_{\mathbf{x}} \xi \\ \nabla_{\mathbf{x}} \eta \\ \nabla_{\mathbf{x}} \varsigma \end{bmatrix},$$

where row vectors  $\nabla_{\mathbf{x}} \xi$ ,  $\nabla_{\mathbf{x}} \eta$  and  $\nabla_{\mathbf{x}} \varsigma$  are

$$\nabla_{\mathbf{x}} \xi := \frac{\mathbf{x}_{\eta}^{\top} \times \mathbf{x}_{\varsigma}^{\top}}{\sqrt{g}}, \quad \nabla_{\mathbf{x}} \eta := \frac{\mathbf{x}_{\varsigma}^{\top} \times \mathbf{x}_{\xi}^{\top}}{\sqrt{g}}, \quad \nabla_{\mathbf{x}} \varsigma := \frac{\mathbf{x}_{\xi}^{\top} \times \mathbf{x}_{\eta}^{\top}}{\sqrt{g}}.$$

The inverse Jacobian (determinant of the inverse Jacobian matrix) is the reciprocal of the Jacobian,

$$\det(\mathcal{J}^{-1}) = \frac{1}{\det(\mathcal{J})},$$

and the inverse metric matrix is expressed as

$$\mathbf{g}^{-1} = \begin{bmatrix} g^{1,1} & g^{1,2} & g^{1,3} \\ g^{2,1} & g^{2,2} & g^{2,3} \\ g^{3,1} & g^{3,2} & g^{3,3} \end{bmatrix} = \mathcal{J}^{-1} (\mathcal{J}^{-1})^{\top},$$

where, to be more explicit,

$$g^{i,j} = \sum_{l=1}^3 \mathcal{J}^{-1}|_{i,l} \mathcal{J}^{-1}|_{j,l}, \quad i, j \in \{1, 2, 3\}.$$

The inverse metric matrix is also symmetric and positive definite. For a comprehensive introduction on coordinate transformation, see for example [131].

**Complement 2.7** For a Python implementation of computing these metric related values and matrices of a given mapping, see script [coordinate\_transformation.py] [www.mathischeap.com/contents/LIBRARY/ptc/coordinate\\_transformation](http://www.mathischeap.com/contents/LIBRARY/ptc/coordinate_transformation).

**Node basis functions** Transforming a discrete node polynomial,  $\psi_0^h \in \text{NP}_N(\Omega_{\text{ref}})$ , to  $\Omega$  can be conducted by

$$\psi^h(x, y, z) = \psi^h(\Phi(\xi, \eta, \varsigma)) = \psi_0^h(\xi, \eta, \varsigma).$$

If we apply this transformation to the basis node polynomials in the reference domain, we obtain the following node basis functions,

$$\text{III}_{\Phi}^{i,j,k}(x, y, z) = \text{III}_{\Phi}^{i,j,k}(\Phi(\xi, \eta, \varsigma)) = \text{III}^{i,j,k}(\xi, \eta, \varsigma), \quad i, j, k \in \{0, 1, \dots, N\},$$

in  $\Omega$ . If we define points

$$(2.66) \quad \mathbf{P}_{l,m,n}^{\Phi} = \Phi(\mathbf{P}_{l,m,n}), \quad l, m, n \in \{0, 1, \dots, N\},$$

where  $P_{l,m,n}$  are the points on which the node polynomials in the reference domain are constructed, see (2.28), we can easily find that the node basis functions  $\mathbb{ll}_{\Phi}^{i,j,k}(x, y, z)$  satisfy the Kronecker delta property expressed as

$$(2.67) \quad \mathbb{ll}_{\Phi}^{i,j,k}(P_{l,m,n}^{\Phi}) = \delta_{l,m,n}^{i,j,k}.$$

Spanned by these node basis functions,  $\text{NP}_N(\Omega)$  is the space of node functions in  $\Omega$ , i.e.,

$$\text{NP}_N(\Omega) := \text{span} \left( \left\{ \mathbb{ll}_{\Phi}^{i,j,k}(\xi, \eta, \varsigma) \mid i, j, k \in \{0, 1, \dots, N\} \right\} \right).$$

**Edge basis functions** Transforming a discrete edge polynomial,  $\omega_0^h \in \text{EP}_{N-1}(\Omega_{\text{ref}})$ , to  $\Omega$  can be done as

$$\omega^h(x, y, z) = \omega^h(\Phi(\xi, \eta, \varsigma)) = (\mathcal{J}^{-1})^{\top} \omega_0^h(\xi, \eta, \varsigma).$$

If we apply this transformation to the basis edge polynomials in the reference domain, we obtain a set of edge basis functions in  $\Omega$ ,

$$\begin{aligned} \mathbf{ell}_{\Phi}^{i,j,k}(x, y, z) &= (\mathcal{J}^{-1})^{\top} \begin{bmatrix} \text{ell}^{i,j,k}(\Phi^{-1}(x, y, z)) \\ 0 \\ 0 \end{bmatrix}, \quad i \in \{1, 2, \dots, N\}, \quad j, k \in \{0, 1, \dots, N\}, \\ \mathbf{lel}_{\Phi}^{i,j,k}(x, y, z) &= (\mathcal{J}^{-1})^{\top} \begin{bmatrix} 0 \\ \text{lel}^{i,j,k}(\Phi^{-1}(x, y, z)) \\ 0 \end{bmatrix}, \quad j \in \{1, 2, \dots, N\}, \quad i, k \in \{0, 1, \dots, N\}, \\ \mathbf{lle}_{\Phi}^{i,j,k}(x, y, z) &= (\mathcal{J}^{-1})^{\top} \begin{bmatrix} 0 \\ 0 \\ \text{lle}^{i,j,k}(\Phi^{-1}(x, y, z)) \end{bmatrix}, \quad k \in \{1, 2, \dots, N\}, \quad i, j \in \{0, 1, \dots, N\}. \end{aligned}$$

And if we define edges  $E_{l,m,n}^{\Phi,\xi}$ ,  $E_{l,m,n}^{\Phi,\eta}$  and  $E_{l,m,n}^{\Phi,\varsigma}$  as the mapped edges of  $E_{l,m,n}^{\xi}$ ,  $E_{l,m,n}^{\eta}$  and  $E_{l,m,n}^{\varsigma}$ , see (2.33), i.e.,

$$(2.68a) \quad E_{l,m,n}^{\Phi,\xi} := \Phi(E_{l,m,n}^{\xi}), \quad l \in \{1, 2, \dots, N\}, \quad m, n \in \{0, 1, \dots, N\},$$

$$(2.68b) \quad E_{l,m,n}^{\Phi,\eta} := \Phi(E_{l,m,n}^{\eta}), \quad m \in \{1, 2, \dots, N\}, \quad l, n \in \{0, 1, \dots, N\},$$

$$(2.68c) \quad E_{l,m,n}^{\Phi,\varsigma} := \Phi(E_{l,m,n}^{\varsigma}), \quad n \in \{1, 2, \dots, N\}, \quad l, m \in \{0, 1, \dots, N\},$$

we will find that the edge basis functions satisfy Kronecker delta properties expressed as

$$(2.69a) \quad \int_{E_{l,m,n}^{\Phi,\xi}} \mathbf{ell}_{\Phi}^{i,j,k} \cdot d\mathbf{r} = \delta_{l,m,n}^{i,j,k}, \quad \int_{E_{l,m,n}^{\Phi,\eta}} \mathbf{ell}_{\Phi}^{i,j,k} \cdot d\mathbf{r} = 0, \quad \int_{E_{l,m,n}^{\Phi,\varsigma}} \mathbf{ell}_{\Phi}^{i,j,k} \cdot d\mathbf{r} = 0,$$

$$(2.69b) \quad \int_{E_{l,m,n}^{\Phi,\xi}} \mathbf{lel}_{\Phi}^{i,j,k} \cdot d\mathbf{r} = 0, \quad \int_{E_{l,m,n}^{\Phi,\eta}} \mathbf{lel}_{\Phi}^{i,j,k} \cdot d\mathbf{r} = \delta_{l,m,n}^{i,j,k}, \quad \int_{E_{l,m,n}^{\Phi,\varsigma}} \mathbf{lel}_{\Phi}^{i,j,k} \cdot d\mathbf{r} = 0,$$

$$(2.69c) \quad \int_{E_{l,m,n}^{\Phi,\xi}} \mathbf{lle}_{\Phi}^{i,j,k} \cdot d\mathbf{r} = 0, \quad \int_{E_{l,m,n}^{\Phi,\eta}} \mathbf{lle}_{\Phi}^{i,j,k} \cdot d\mathbf{r} = 0, \quad \int_{E_{l,m,n}^{\Phi,\varsigma}} \mathbf{lle}_{\Phi}^{i,j,k} \cdot d\mathbf{r} = \delta_{l,m,n}^{i,j,k}.$$

We use  $\text{EP}_{N-1}(\Omega)$  to denote the space of edge functions in  $\Omega$ , i.e.,

$$\begin{aligned} \text{EP}_{N-1}(\Omega) &:= \\ &\text{span} \left( \left\{ \dots, \mathbf{ell}_{\Phi}^{i,j,k}(\xi, \eta, \varsigma), \dots \right\} \cup \left\{ \dots, \mathbf{lel}_{\Phi}^{i,j,k}(\xi, \eta, \varsigma), \dots \right\} \cup \left\{ \dots, \mathbf{lle}_{\Phi}^{i,j,k}(\xi, \eta, \varsigma), \dots \right\} \right). \end{aligned}$$

**Face basis functions** Transforming a discrete face polynomial,  $\mathbf{u}_0^h \in \text{FP}_{N-1}(\Omega_{\text{ref}})$ , to  $\Omega$  can be done through

$$\mathbf{u}^h(x, y, z) = \mathbf{u}^h(\Phi(\xi, \eta, \varsigma)) = \frac{\mathcal{J}}{\sqrt{g}} \mathbf{u}_0^h(\xi, \eta, \varsigma),$$

If we apply this transformation to the basis face polynomials in the reference domain, we obtain a set of face basis functions in  $\Omega$ ,

$$\begin{aligned} \mathbf{lee}_{\Phi}^{i,j,k}(x, y, z) &= \frac{\mathcal{J}}{\sqrt{g}} \begin{bmatrix} \mathbf{lee}^{i,j,k}(\Phi^{-1}(x, y, z)) \\ 0 \\ 0 \end{bmatrix}, \quad i \in \{0, 1, \dots, N\}, \quad j, k \in \{1, 2, \dots, N\}, \\ \mathbf{ele}_{\Phi}^{i,j,k}(x, y, z) &= \frac{\mathcal{J}}{\sqrt{g}} \begin{bmatrix} 0 \\ \mathbf{ele}^{i,j,k}(\Phi^{-1}(x, y, z)) \\ 0 \end{bmatrix}, \quad j \in \{0, 1, \dots, N\}, \quad i, k \in \{1, 2, \dots, N\}, \\ \mathbf{eel}_{\Phi}^{i,j,k}(x, y, z) &= \frac{\mathcal{J}}{\sqrt{g}} \begin{bmatrix} 0 \\ 0 \\ \mathbf{eel}^{i,j,k}(\Phi^{-1}(x, y, z)) \end{bmatrix}, \quad k \in \{0, 1, \dots, N\}, \quad i, j \in \{1, 2, \dots, N\}. \end{aligned}$$

And if we define faces  $F_{l,m,n}^{\Phi,\xi}$ ,  $F_{l,m,n}^{\Phi,\eta}$  and  $F_{l,m,n}^{\Phi,\varsigma}$  as the mapped faces of  $F_{l,m,n}^{\xi}$ ,  $F_{l,m,n}^{\eta}$  and  $F_{l,m,n}^{\varsigma}$ , see (2.38), i.e.,

$$(2.70a) \quad F_{l,m,n}^{\Phi,\xi} := \Phi(F_{l,m,n}^{\xi}), \quad l \in \{0, 1, \dots, N\}, \quad m, n \in \{1, 2, \dots, N\},$$

$$(2.70b) \quad F_{l,m,n}^{\Phi,\eta} := \Phi(F_{l,m,n}^{\eta}), \quad m \in \{0, 1, \dots, N\}, \quad l, n \in \{1, 2, \dots, N\},$$

$$(2.70c) \quad F_{l,m,n}^{\Phi,\varsigma} := \Phi(F_{l,m,n}^{\varsigma}), \quad n \in \{0, 1, \dots, N\}, \quad l, m \in \{1, 2, \dots, N\},$$

we can find that the face basis functions satisfy Kronecker delta properties expressed as

$$(2.71a) \quad \int_{F_{l,m,n}^{\Phi,\xi}} \mathbf{lee}_{\Phi}^{i,j,k} \cdot d\mathbf{A} = \delta_{l,m,n}^{i,j,k}, \quad \int_{F_{l,m,n}^{\Phi,\eta}} \mathbf{lee}_{\Phi}^{i,j,k} \cdot d\mathbf{A} = 0, \quad \int_{F_{l,m,n}^{\Phi,\varsigma}} \mathbf{lee}_{\Phi}^{i,j,k} \cdot d\mathbf{A} = 0,$$

$$(2.71b) \quad \int_{F_{l,m,n}^{\Phi,\xi}} \mathbf{ele}_{\Phi}^{i,j,k} \cdot d\mathbf{A} = 0, \quad \int_{F_{l,m,n}^{\Phi,\eta}} \mathbf{ele}_{\Phi}^{i,j,k} \cdot d\mathbf{A} = \delta_{l,m,n}^{i,j,k}, \quad \int_{F_{l,m,n}^{\Phi,\varsigma}} \mathbf{ele}_{\Phi}^{i,j,k} \cdot d\mathbf{A} = 0,$$

$$(2.71c) \quad \int_{F_{l,m,n}^{\Phi,\xi}} \mathbf{eel}_{\Phi}^{i,j,k} \cdot d\mathbf{A} = 0, \quad \int_{F_{l,m,n}^{\Phi,\eta}} \mathbf{eel}_{\Phi}^{i,j,k} \cdot d\mathbf{A} = 0, \quad \int_{F_{l,m,n}^{\Phi,\varsigma}} \mathbf{eel}_{\Phi}^{i,j,k} \cdot d\mathbf{A} = \delta_{l,m,n}^{i,j,k}.$$

and we use  $\text{FP}_{N-1}(\Omega)$  to denote the space of face functions in  $\Omega$ , i.e.,

$$\begin{aligned} \text{FP}_{N-1}(\Omega) &:= \\ &\text{span} \left( \left\{ \dots, \mathbf{lee}_{\Phi}^{i,j,k}(\xi, \eta, \varsigma), \dots \right\} \cup \left\{ \dots, \mathbf{ele}_{\Phi}^{i,j,k}(\xi, \eta, \varsigma), \dots \right\} \cup \left\{ \dots, \mathbf{eel}_{\Phi}^{i,j,k}(\xi, \eta, \varsigma), \dots \right\} \right). \end{aligned}$$

**Volume basis functions** Transforming a discrete volume polynomial,  $f_0^h \in \text{VP}_{N-1}(\Omega_{\text{ref}})$ , to  $\Omega$  can be conducted by

$$f^h(x, y, z) = f^h(\Phi(\xi, \eta, \varsigma)) = \frac{1}{\sqrt{g}} f_0^h(\xi, \eta, \varsigma),$$

If we apply this transformation to the basis volume polynomials in the reference domain, we obtain a set of volume basis functions in  $\Omega$ ,

$$\text{eee}_{\Phi}^{i,j,k}(x, y, z) = \text{eee}_{\Phi}^{i,j,k}(\Phi(\xi, \eta, \varsigma)) = \frac{1}{\sqrt{g}} \text{eee}^{i,j,k}(\xi, \eta, \varsigma), \quad i, j, k \in \{1, 2, \dots, N\}.$$

If we define volumes  $V_{l,m,n}^{\Phi}$  as the mapped volumes of  $V_{l,m,n}$ , see (2.42), namely,

$$(2.72) \quad V_{l,m,n}^{\Phi} := \Phi(V_{l,m,n}), \quad l, m, n \in \{1, 2, \dots, N\},$$

we will find the following Kronecker delta property for the volume basis functions,

$$(2.73) \quad \int_{V_{l,m,n}^{\Phi}} \text{eee}_{\Phi}^{i,j,k}(x, y, z) dV = \delta_{l,m,n}^{i,j,k}.$$

We now define  $\text{VP}_N(\Omega)$ ,

$$\text{VP}_{N-1}(\Omega) := \text{span} \left( \left\{ \text{eee}_{\Phi}^{i,j,k}(\xi, \eta, \varsigma) \mid i, j, k \in \{1, 2, \dots, N\} \right\} \right),$$

as the space of volume functions in  $\Omega$ .

**Complement 2.8** For a proof of Kronecker delta properties (2.67), (2.69), (2.71) and (2.73), see document [Kronecker\_delta.pdf]  
[www.mathischeap.com/contents/LIBRARY/ptc/Kronecker\\_delta](http://www.mathischeap.com/contents/LIBRARY/ptc/Kronecker_delta).

※ Discrete functions in spaces  $\text{NP}_N(\Omega)$ ,  $\text{EP}_{N-1}(\Omega)$ ,  $\text{FP}_{N-1}(\Omega)$  and  $\text{VP}_{N-1}(\Omega)$  are of the following forms.

- A node function  $\psi^h \in \text{NP}_N(\Omega)$  is of the form

$$(2.74) \quad \psi^h(x, y, z) = \sum_{i=0}^N \sum_{j=0}^N \sum_{k=0}^N \Psi_{i,j,k} \text{lll}_{\Phi}^{i,j,k}(x, y, z).$$

where  $\Psi_{i,j,k} \in \mathbb{R}$  are the expansion coefficients of the node function. And from the Kronecker delta property (2.67), we have

$$(2.75) \quad \psi^h(P_{l,m,n}^{\Phi}) = \Psi_{l,m,n}.$$

- A edge function  $\omega^h \in \text{EP}_{N-1}(\Omega)$  is of the form

$$(2.76) \quad \begin{aligned} \omega^h(x, y, z) = & \sum_{i=1}^N \sum_{j=0}^N \sum_{k=0}^N w_{i,j,k}^{\xi} \text{ell}_{\Phi}^{i,j,k}(x, y, z) \\ & + \sum_{i=0}^N \sum_{j=1}^N \sum_{k=0}^N w_{i,j,k}^{\eta} \text{lel}_{\Phi}^{i,j,k}(x, y, z) \\ & + \sum_{i=0}^N \sum_{j=0}^N \sum_{k=1}^N w_{i,j,k}^{\varsigma} \text{lle}_{\Phi}^{i,j,k}(x, y, z). \end{aligned}$$

where  $w_{i,j,k}^\xi, w_{i,j,k}^\eta, w_{i,j,k}^\zeta \in \mathbb{R}$  are the expansion coefficients of the edge function. And from Kronecker delta properties (2.69), we find that

$$(2.77a) \quad \int_{E_{l,m,n}^{\Phi,\xi}} \boldsymbol{\omega}^h \cdot d\mathbf{r} = w_{l,m,n}^\xi,$$

$$(2.77b) \quad \int_{E_{l,m,n}^{\Phi,\eta}} \boldsymbol{\omega}^h \cdot d\mathbf{r} = w_{l,m,n}^\eta,$$

$$(2.77c) \quad \int_{E_{l,m,n}^{\Phi,\zeta}} \boldsymbol{\omega}^h \cdot d\mathbf{r} = w_{l,m,n}^\zeta.$$

- A face function  $\mathbf{u}^h \in \text{FP}_{N-1}(\Omega)$  is of the form

$$(2.78) \quad \begin{aligned} \mathbf{u}^h(x, y, z) &= \sum_{i=0}^N \sum_{j=1}^N \sum_{k=1}^N u_{i,j,k}^\xi \mathbf{lee}_{\Phi}^{i,j,k}(x, y, z) \\ &+ \sum_{i=1}^N \sum_{j=0}^N \sum_{k=1}^N u_{i,j,k}^\eta \mathbf{ele}_{\Phi}^{i,j,k}(x, y, z) \\ &+ \sum_{i=1}^N \sum_{j=1}^N \sum_{k=0}^N u_{i,j,k}^\zeta \mathbf{eel}_{\Phi}^{i,j,k}(x, y, z) \end{aligned}$$

where  $u_{i,j,k}^\xi, u_{i,j,k}^\eta, u_{i,j,k}^\zeta \in \mathbb{R}$  are the expansion coefficients of the face function. And from Kronecker delta properties (2.71), we obtain that

$$(2.79a) \quad \int_{F_{l,m,n}^{\Phi,\xi}} \mathbf{u}^h \cdot d\mathbf{A} = u_{l,m,n}^\xi,$$

$$(2.79b) \quad \int_{F_{l,m,n}^{\Phi,\eta}} \mathbf{u}^h \cdot d\mathbf{A} = u_{l,m,n}^\eta,$$

$$(2.79c) \quad \int_{F_{l,m,n}^{\Phi,\zeta}} \mathbf{u}^h \cdot d\mathbf{A} = u_{l,m,n}^\zeta.$$

- A volume function  $f^h \in \text{VP}_{N-1}(\Omega)$  is of the form

$$(2.80) \quad f^h(x, y, z) = \sum_{i=1}^N \sum_{j=1}^N \sum_{k=1}^N f_{i,j,k} \mathbf{eee}_{\Phi}^{i,j,k}(x, y, z),$$

where  $f_{i,j,k} \in \mathbb{R}$  are the expansion coefficients of the volume function. And from the Kronecker delta property (2.73), we will find

$$(2.81) \quad \int_{V_{l,m,n}^{\Phi}} f^h dV = f_{l,m,n}.$$

Recall that the indexings and local numberings for the reference domain have been inherited in the general domain  $\Omega$ . We now repeat the analysis that has been done for the reference domain in Section 2.3.2 except that this time we integrate over the mapped geometric objects, see (2.66), (2.68), (2.70) and (2.72) (instead of the original geometric objects) and use the properties (2.75), (2.77), (2.79) and (2.81) for the general domain (instead of the ones, see (2.45), (2.46), (2.47)

and (2.48), for the reference domain). And we again use the gradient theorem for line integrals, the Stokes' integral theorem and the Gauss' integral theorem. As a result, we can find that the gradient, curl and divergence operators for spaces  $\text{NP}_N(\Omega)$ ,  $\text{EP}_{N-1}(\Omega)$  and  $\text{FP}_{N-1}(\Omega)$  will still have the same exact, topological discrete counterparts, the incidence matrices  $\mathbf{E}_{(\nabla)}$ ,  $\mathbf{E}_{(\nabla \times)}$  and  $\mathbf{E}_{(\nabla \cdot)}$  as those derived in Section 2.3.2 for the reference domain regardless of the mapping  $\Phi$ .

Having found the incidence matrices for the general domain, once again, we can follow the same analysis for (2.25) and obtain

$$\begin{aligned} \nabla \psi^h &\in \text{EP}_{N-1}(\Omega) & \forall \psi^h &\in \text{NP}_N(\Omega), \\ \nabla \times \boldsymbol{\omega}^h &\in \text{FP}_{N-1}(\Omega) & \forall \boldsymbol{\omega}^h &\in \text{EP}_{N-1}(\Omega), \\ \nabla \cdot \mathbf{u}^h &\in \text{VP}_{N-1}(\Omega) & \forall \mathbf{u}^h &\in \text{FP}_{N-1}(\Omega). \end{aligned}$$

Thus, we can conclude that the mimetic spaces  $\text{NP}_N(\Omega)$ ,  $\text{EP}_{N-1}(\Omega)$ ,  $\text{FP}_{N-1}(\Omega)$  and  $\text{VP}_{N-1}(\Omega)$  form the following discrete de Rham complex,

$$(2.82) \quad \begin{array}{ccc} \text{NP}_N(\Omega) & \subset & H^1(\Omega) \\ \downarrow \nabla & & \downarrow \nabla \\ \text{EP}_{N-1}(\Omega) & \subset & H(\text{curl}; \Omega) \\ \downarrow \nabla \times & & \downarrow \nabla \times \\ \text{FP}_{N-1}(\Omega) & \subset & H(\text{div}; \Omega) \\ \downarrow \nabla \cdot & & \downarrow \nabla \cdot \\ \text{VP}_{N-1}(\Omega) & \subset & L^2(\Omega) \end{array},$$

where the gradient, curl and divergence operators still have the exact discrete counterparts, the incidence matrices  $\mathbf{E}_{(\nabla)}$ ,  $\mathbf{E}_{(\nabla \times)}$  and  $\mathbf{E}_{(\nabla \cdot)}$  which are topological and thus do not depend on the mapping  $\Phi$ . This is consistent with the statement that the MSEM preserves the topological structure of primal operators at the discrete level. The subscripts,  $N$  and  $N - 1$ , of these spaces refer to the overall degrees of the corresponding polynomials in the reference domain, and we call  $\text{NP}_N(\Omega)$ ,  $\text{EP}_{N-1}(\Omega)$ ,  $\text{FP}_{N-1}(\Omega)$  and  $\text{VP}_{N-1}(\Omega)$  a set of mimetic spaces of degree  $N$ .

※ Given a variable, i.e.,  $\psi \in H^1(\Omega)$ ,  $\boldsymbol{\omega} \in H(\text{curl}; \Omega)$ ,  $\mathbf{u} \in H(\text{div}; \Omega)$  or  $f \in L^2(\Omega)$ , we can find its projection in  $\text{NP}_N(\Omega)$ ,  $\text{EP}_{N-1}(\Omega)$ ,  $\text{FP}_{N-1}(\Omega)$  or  $\text{VP}_{N-1}(\Omega)$  through the projection operator [33, 83],

$$\pi := \mathcal{I} \circ \mathcal{R},$$

where  $\mathcal{R}$  is the *reduction* operator which takes the variable and produces the expansion coefficients and  $\mathcal{I}$  is the *reconstruction* operator which reconstructs the discrete variable with the expansion coefficients as a linear combinations of corresponding basis functions, i.e., the mimetic basis functions in this case. Particular projections are explained as follows:

- For  $\psi \in H^1(\Omega)$ , the expansion coefficients of its projection  $\psi^h := \pi(\psi) \in \text{NP}_N(\Omega)$ , are

$$(2.83) \quad \Psi_{i,j,k} = \psi(P_{i,j,k}^\Phi),$$

where points  $P_{i,j,k}^\Phi$  are the mapped points, see (2.66). For the form of the discrete variable  $\phi^h$ , see (2.74).

- For  $\boldsymbol{\omega} \in H(\text{curl}; \Omega)$ , the expansion coefficients of its projection  $\boldsymbol{\omega}^h := \pi(\boldsymbol{\omega}) \in \text{EP}_{N-1}(\Omega)$  are

$$(2.84a) \quad \mathbf{w}_{i,j,k}^\xi = \int_{E_{i,j,k}^{\Phi,\xi}} \boldsymbol{\omega} \cdot d\mathbf{r}$$

$$(2.84b) \quad \mathbf{w}_{i,j,k}^\eta = \int_{E_{i,j,k}^{\Phi,\eta}} \boldsymbol{\omega} \cdot d\mathbf{r}$$

$$(2.84c) \quad \mathbf{w}_{i,j,k}^\varsigma = \int_{E_{i,j,k}^{\Phi,\varsigma}} \boldsymbol{\omega} \cdot d\mathbf{r},$$

where edges  $E_{i,j,k}^{\Phi,\xi}$ ,  $E_{i,j,k}^{\Phi,\eta}$  and  $E_{i,j,k}^{\Phi,\varsigma}$  are the mapped edges, see (2.68). For the form of the discrete variable  $\boldsymbol{\omega}^h$ , see (2.76).

- For  $\mathbf{u} \in H(\text{div}; \Omega)$ , the expansion coefficients of its projection  $\mathbf{u}^h := \pi(\mathbf{u}) \in \text{FP}_{N-1}(\Omega)$  are

$$(2.85a) \quad \mathbf{u}_{i,j,k}^\xi = \int_{S_{i,j,k}^{\Phi,\xi}} \mathbf{u} \cdot d\mathbf{A},$$

$$(2.85b) \quad \mathbf{u}_{i,j,k}^\eta = \int_{S_{i,j,k}^{\Phi,\eta}} \mathbf{u} \cdot d\mathbf{A},$$

$$(2.85c) \quad \mathbf{u}_{i,j,k}^\varsigma = \int_{S_{i,j,k}^{\Phi,\varsigma}} \mathbf{u} \cdot d\mathbf{A},$$

where edges  $S_{i,j,k}^{\Phi,\xi}$ ,  $S_{i,j,k}^{\Phi,\eta}$  and  $S_{i,j,k}^{\Phi,\varsigma}$  are the mapped faces, see (2.70). For the form of the discrete variable  $\mathbf{u}^h$ , see (2.78).

- For  $f \in L^2(\Omega)$ , the expansion coefficients of its projection  $f^h := \pi(f) \in \text{VP}_{N-1}(\Omega)$  are

$$(2.86) \quad \mathbf{f}_{i,j,k} = \int_{V_{i,j,k}^\Phi} f \, dV,$$

where volumes  $V_{i,j,k}^\Phi$  are the mapped volumes, see (2.72). For the form of the discrete variable  $f^h$ , see (2.80).

Note that we have assumed that integrals (2.83), (2.84), (2.85) and (2.86), i.e., the reductions, exist. For more discussions about the well-posedness of the reduction operator, we refer to, for example, [34, 83, 112].

**Complement 2.9** For a Python implementation of these projections, see script [projection.py] [www.mathischeap.com/contents/LIBRARY/ptc/projection](http://www.mathischeap.com/contents/LIBRARY/ptc/projection).

We can assess the accuracy of the projection by measuring the  $L^2$ -error, for example,

$$\left\| \boldsymbol{\psi}^h \right\|_{L^2\text{-error}} := \left\| \boldsymbol{\psi}^h - \boldsymbol{\psi} \right\|_{L^2},$$

$$\left\| \mathbf{u}^h \right\|_{L^2\text{-error}} := \left\| \mathbf{u}^h - \mathbf{u} \right\|_{L^2},$$

where  $\|\cdot\|_{L^2}$  is the  $L^2$ -norm, namely,  $\|\cdot\|_{L^2} = \sqrt{\langle \cdot, \cdot \rangle_\Omega}$ .

**Complement 2.10** For a Python implementation of computing the  $L^2$ -error, see script [L2\_error.py] [www.mathischeap.com/contents/LIBRARY/ptc/L2\\_error](http://www.mathischeap.com/contents/LIBRARY/ptc/L2_error).

※ The  $L^2$ -inner product of two elements from these spaces can be calculated in the following ways.

- For two discrete functions  $p^h, \psi^h \in \text{NP}_N(\Omega)$ , the  $L^2$ -inner product of them is

$$(2.87) \quad \langle p^h, \psi^h \rangle_\Omega = \underline{p}^\top \mathbf{M}_N \underline{\psi} = \underline{\psi}^\top \mathbf{M}_N \underline{p},$$

where  $\mathbf{M}_N$  is the mass matrix of space  $\text{NP}_N(\Omega)$  and is symmetric and positive definite.

- For two discrete functions  $\mathbf{q}^h, \boldsymbol{\omega}^h \in \text{EP}_{N-1}(\Omega)$ , the  $L^2$ -inner product of them is

$$(2.88) \quad \langle \mathbf{q}^h, \boldsymbol{\omega}^h \rangle_\Omega = \underline{\mathbf{q}}^\top \mathbf{M}_E \underline{\boldsymbol{\omega}} = \underline{\boldsymbol{\omega}}^\top \mathbf{M}_E \underline{\mathbf{q}},$$

where  $\mathbf{M}_E$  is the mass matrix of space  $\text{EP}_{N-1}(\Omega)$  and is symmetric and positive definite.

- For two discrete functions  $\mathbf{v}^h, \mathbf{u}^h \in \text{FP}_{N-1}(\Omega)$ , the  $L^2$ -inner product of them is

$$(2.89) \quad \langle \mathbf{v}^h, \mathbf{u}^h \rangle_\Omega = \underline{\mathbf{v}}^\top \mathbf{M}_F \underline{\mathbf{u}} = \underline{\mathbf{u}}^\top \mathbf{M}_F \underline{\mathbf{v}},$$

where  $\mathbf{M}_F$  is the mass matrix of space  $\text{EP}_{N-1}(\Omega)$  and is symmetric and positive definite.

- For two discrete functions  $\phi^h, f^h \in \text{VP}_{N-1}(\Omega)$ , we have

$$(2.90) \quad \langle \phi^h, f^h \rangle_\Omega = \underline{\phi}^\top \mathbf{M}_V \underline{f} = \underline{f}^\top \mathbf{M}_V \underline{\phi},$$

where  $\mathbf{M}_V$  is the mass matrix of the space  $\text{VP}_{N-1}(\Omega)$  and is symmetric and positive definite.

Recall that we use underlined symbols to indicate vectors of expansion coefficients of discrete elements, for example,  $\underline{p}$ ,  $\underline{\psi}$ ,  $\underline{\boldsymbol{\omega}}$ ,  $\underline{\mathbf{u}}$ ,  $\underline{f}$  and so on.

**Complement 2.11** For an instruction of how to compute the entries of mass matrices  $\mathbf{M}_N$ ,  $\mathbf{M}_E$ ,  $\mathbf{M}_F$  and  $\mathbf{M}_V$ , see document [mass\_matrices.pdf] [www.mathischeap.com/contents/LIBRARY/ptc/mass\\_matrices\\_pdf](http://www.mathischeap.com/contents/LIBRARY/ptc/mass_matrices_pdf).

**Complement 2.12** For a Python implementation of calculating mass matrices  $\mathbf{M}_N$ ,  $\mathbf{M}_E$ ,  $\mathbf{M}_F$  and  $\mathbf{M}_V$  under a given mapping, see script [mass\_matrices.py] [www.mathischeap.com/contents/LIBRARY/ptc/mass\\_matrices\\_py](http://www.mathischeap.com/contents/LIBRARY/ptc/mass_matrices_py).

When a material parameter is involved in the  $L^2$ -inner product, the material property can be embedded by the mass matrix. For example,

$$\langle \mathbf{v}^h, k^{-1} \mathbf{u}^h \rangle_\Omega = \underline{\mathbf{v}}^\top \mathbf{M}_F^k \underline{\mathbf{u}}.$$

## 2.4 Application to the Poisson problem

In this section, we demonstrate the MSEM by applying it to the Poisson problem.

### 2.4.1 Single element case

For convenience, here we briefly repeat the weak formulation (2.15): Given  $f \in L^2(\Omega)$ ,  $\widehat{\varphi} \in H^{1/2}(\Gamma_\varphi)$  and  $\widehat{\mathbf{u}} \in H^{-1/2}(\Gamma_{\mathbf{u}})$ , seek  $(\mathbf{u}, \varphi) \in H_{\widehat{\mathbf{u}}}(\text{div}; \Omega) \times L^2(\Omega)$  such that

$$(2.91a) \quad \langle \mathbf{v}, k^{-1} \mathbf{u} \rangle_\Omega + \langle \nabla \cdot \mathbf{v}, \varphi \rangle_\Omega = \int_{\Gamma_\varphi} \widehat{\varphi} (\mathbf{v} \cdot \mathbf{n}) \, d\Gamma \quad \forall \mathbf{v} \in H_0(\text{div}; \Omega),$$

$$(2.91b) \quad \langle \phi, \nabla \cdot \mathbf{u} \rangle_\Omega = - \langle \phi, f \rangle_\Omega \quad \forall \phi \in L^2(\Omega).$$

Assume we are in  $\mathbb{R}^3$  and there is a smooth enough mapping  $\Phi$ , see (2.65), which maps  $\Omega_{\text{ref}}$  into  $\Omega$ . In other words, we consider the whole computational domain as a single element. Mimetic spaces  $\text{NP}_N(\Omega)$ ,  $\text{EP}_{N-1}(\Omega)$ ,  $\text{FP}_{N-1}(\Omega)$  and  $\text{VP}_{N-1}(\Omega)$  then can be constructed in the computational domain. We use  $\text{FP}_{N-1}(\Omega)$  to approximate space  $H(\text{div}; \Omega)$  and use  $\text{VP}_{N-1}(\Omega)$  to approximate space  $L^2(\Omega)$ , i.e., in the discrete de Rham complex (2.82), we take

$$\begin{array}{ccc} \text{FP}_{N-1}(\Omega) & \subset & H(\text{div}; \Omega) \\ \downarrow \nabla \cdot & & \downarrow \nabla \cdot \\ \text{VP}_{N-1}(\Omega) & \subset & L^2(\Omega) \end{array} ,$$

If we set boundaries  $\Gamma_\varphi$  and  $\Gamma_{\mathbf{u}}$  to  $\Gamma_\varphi = \partial\Omega$  and  $\Gamma_{\mathbf{u}} = \emptyset$ , a discrete version of (2.91) can be written as: Given  $f \in L^2(\Omega)$ , seek  $(\mathbf{u}^h, \varphi^h) \in \text{FP}_{N-1}(\Omega) \times \text{VP}_{N-1}(\Omega)$  such that

$$(2.92a) \quad \langle \mathbf{v}^h, k^{-1} \mathbf{u}^h \rangle_\Omega + \langle \nabla \cdot \mathbf{v}^h, \varphi^h \rangle_\Omega = \int_{\partial\Omega} \widehat{\varphi} (\mathbf{v}^h \cdot \mathbf{n}) \, d\Gamma \quad \forall \mathbf{v}^h \in \text{FP}_{N-1}(\Omega),$$

$$(2.92b) \quad \langle \phi^h, \nabla \cdot \mathbf{u}^h \rangle_\Omega = - \langle \phi^h, f^h \rangle_\Omega \quad \forall \phi^h \in \text{VP}_{N-1}(\Omega).$$

**Remark 2.3** *Note that, in the boundary integral term of (2.92a),  $\widehat{\varphi}$  is at the continuous level (without superscript  $h$ ). This is because when it is time to evaluate this boundary integral to include the boundary condition  $\widehat{\varphi}$  (to obtain the entries of vector  $\mathbf{b}$  in (2.93) and (2.94), see Complement 2.13), we could directly use the continuous boundary variable  $\widehat{\varphi}$ . While for  $f \in L^2(\Omega)$  we have projected it into  $f^h \in \text{VP}_{N-1}(\Omega)$  in (2.92b), see (2.86) for how to do this projection.*

The system (2.92) can be written in algebraic format as

$$(2.93a) \quad \underline{\mathbf{v}}^\top \mathbf{M}_F^k \underline{\mathbf{u}} + \underline{\mathbf{v}}^\top \mathbf{E}_{(\nabla \cdot)}^\top \mathbf{M}_V \underline{\varphi} = \underline{\mathbf{v}}^\top \mathbf{b} \quad \forall \underline{\mathbf{v}} \in \mathbb{R}^{3N^2(N+1)},$$

$$(2.93b) \quad \underline{\phi}^\top \mathbf{M}_V \mathbf{E}_{(\nabla \cdot)} \underline{\mathbf{u}} = - \underline{\phi}^\top \mathbf{M}_V \underline{f} \quad \forall \underline{\phi} \in \mathbb{R}^{N^3}.$$

which is equivalent to a linear system,

$$(2.94) \quad \begin{bmatrix} \mathbf{M}_F^k & \mathbf{E}_{(\nabla \cdot)}^\top \mathbf{M}_V \\ \mathbf{M}_V \mathbf{E}_{(\nabla \cdot)} & \mathbf{0} \end{bmatrix} \begin{bmatrix} \underline{\mathbf{u}} \\ \underline{\varphi} \end{bmatrix} = \begin{bmatrix} \mathbf{b} \\ -\mathbf{M}_V \underline{f} \end{bmatrix}.$$

Since we have set boundaries  $\Gamma_\varphi$  and  $\Gamma_{\mathbf{u}}$  to  $\Gamma_\varphi = \partial\Omega$  and  $\Gamma_{\mathbf{u}} = \emptyset$  which is not the true case, we are not able to evaluate all entries of the vector  $\mathbf{b}$ . These unknown entries will later

be eliminated when we include the boundary condition  $\hat{u}$  by making changes in the first block row of (2.94). See Complement 2.13 for an illustration of a practical approach of including the boundary conditions.

**Complement 2.13** For an illustration of a practical approach of including the boundary conditions, see document [boundary\_conditions.pdf]  
[www.mathischeap.com/contents/LIBRARY/ptc/boundary\\_conditions](http://www.mathischeap.com/contents/LIBRARY/ptc/boundary_conditions).

Note that the approach of imposing the boundary conditions introduced here is not the only approach, but is practical and easy for implementation one.

By now, we finally get the discrete linear system ready to solve. Once the system is solved, we can reconstruct the numerical solutions  $(\mathbf{u}^h, \varphi^h) \in \text{FP}_{N-1}(\Omega) \times \text{VP}_{N-1}(\Omega)$  for the Poisson problem with the expansion coefficients in solutions  $\underline{\mathbf{u}}$  and  $\underline{\varphi}$  of the discrete linear system and the corresponding mimetic basis functions.

So far, everything happened in one single element. In practice, cases with multiple elements are more common. We will further demonstrate the usage of the MSEM in a domain divided into multiple elements in the next subsection.

## 2.4.2 A particular example of multiple mesh elements

Now, as a particular example, we apply the MSEM to a Poisson problem with a manufactured solution in a 3D domain divided into multiple elements. The domain is selected to be a unit cube,

$$\Omega = [0, 1]^3,$$

and the manufactured solution is

$$\varphi_{\text{exact}} = \sin(2\pi x) \sin(2\pi y) \sin(2\pi z).$$

If  $\varphi_{\text{exact}}$  solves the Poisson problem with material parameter  $k = 1$ , the exact solution of  $\mathbf{u}$  and the corresponding source term,  $f$ , then can be computed,

$$\mathbf{u}_{\text{exact}} = \nabla \varphi_{\text{exact}} = \begin{bmatrix} 2\pi \cos(2\pi x) \sin(2\pi y) \sin(2\pi z) \\ 2\pi \sin(2\pi x) \cos(2\pi y) \sin(2\pi z) \\ 2\pi \sin(2\pi x) \sin(2\pi y) \cos(2\pi z) \end{bmatrix},$$

$$(2.95) \quad f = -\nabla \cdot \mathbf{u}_{\text{exact}} = 12\pi^2 \sin(2\pi x) \sin(2\pi y) \sin(2\pi z).$$

We select the boundary  $\Gamma_\varphi$  to be the face  $x = 0$ . The complete weak formulation of this particular problem is: In  $\Omega = [0, 1]^3$  with boundary  $\partial\Omega = \Gamma_\varphi \cup \Gamma_{\mathbf{u}}$ , where  $\Gamma_\varphi = (0, (0, 1), (0, 1))$ , given  $f \in L^2(\Omega)$ , boundary conditions  $\hat{\varphi} = \varphi_{\text{exact}}$  on  $\Gamma_\varphi$  and  $\hat{\mathbf{u}} = \mathbf{u}_{\text{exact}} \cdot \mathbf{n}$  on  $\Gamma_{\mathbf{u}}$ , find  $(\mathbf{u}, \varphi) \in H_{\hat{\mathbf{u}}}(\text{div}; \Omega) \times L^2(\Omega)$  such that (2.91) is satisfied.

In  $\Omega$ , a conforming structured mesh of  $K^3$  elements,

$$(2.96) \quad \Omega_m = \Omega_{i+(j-1)K+(k-1)K^2} = \Omega_{i,j,k}, \quad i, j, k \in \{1, 2, \dots, K\},$$

is generated. The mapping  $\Phi_{i,j,k} : \Omega_{\text{ref}} \rightarrow \Omega_{i,j,k}$  is given as

$$\Phi_{i,j,k} = \overset{\circ}{\Phi} \circ \Xi_{i,j,k},$$

where  $\Xi_{i,j,k}$  is a linear mapping,

$$\Xi_{i,j,k} : \Omega_{\text{ref}} \rightarrow \left( \left[ \frac{i-1}{K}, \frac{i}{K} \right], \left[ \frac{j-1}{K}, \frac{j}{K} \right], \left[ \frac{k-1}{K}, \frac{k}{K} \right] \right),$$

i.e.,

$$\begin{pmatrix} r \\ s \\ t \end{pmatrix} = \Xi_{i,j,k}(\xi, \eta, \varsigma) = \frac{1}{K} \begin{pmatrix} i-1 + (\xi+1)/2 \\ j-1 + (\eta+1)/2 \\ k-1 + (\varsigma+1)/2 \end{pmatrix},$$

and  $\mathring{\Phi}$  is a mapping expressed as

$$(2.97) \quad \begin{pmatrix} x \\ y \\ z \end{pmatrix} = \mathring{\Phi}(r, s, t) = \begin{pmatrix} r + \frac{1}{2}c \sin(2\pi r) \sin(2\pi s) \sin(2\pi t) \\ s + \frac{1}{2}c \sin(2\pi r) \sin(2\pi s) \sin(2\pi t) \\ t + \frac{1}{2}c \sin(2\pi r) \sin(2\pi s) \sin(2\pi t) \end{pmatrix},$$

where  $0 \leq c \leq 0.25$  is a deformation factor. When  $c = 0$ ,  $\mathring{\Phi}$  is also linear and, thus, we get a uniform orthogonal mesh. While, when  $c > 0$ , the mesh is curvilinear. We call this mesh the *crazy mesh*. Two examples of the crazy mesh are shown in Fig. 2.6.

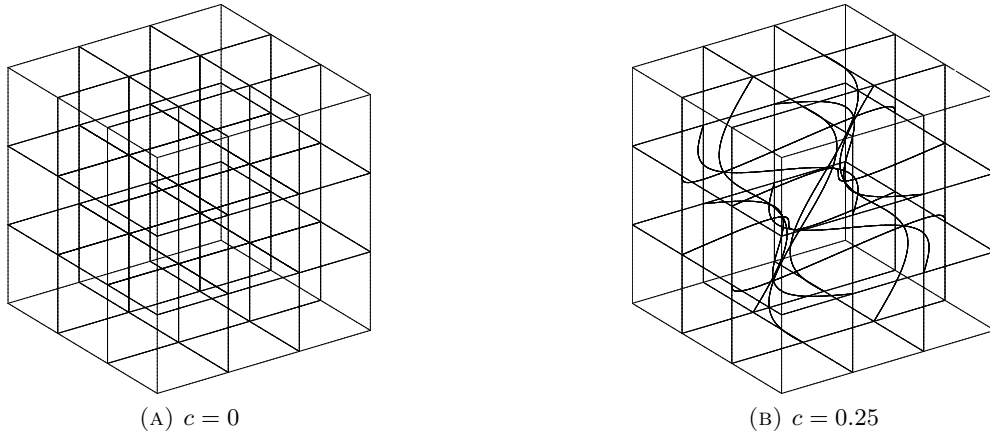


FIGURE 2.6: Two examples of the crazy mesh of  $3^3$  elements.

**Complement 2.14** For a Python implementation of the crazy mesh, see script [crazy\_mesh.py] [www.mathischeap.com/contents/LIBRARY/ptc/crazy\\_mesh](http://www.mathischeap.com/contents/LIBRARY/ptc/crazy_mesh).

We now can apply the discretization introduced in Section 2.4.1 to all elements of the mesh and obtain  $K^3$  local linear systems. Assembling these local systems leads to a global discrete linear algebra system ready to be solved. And we denote the left-hand side matrix of the global matrix by  $\mathbb{F}$ . For an introduction of the assembly of local systems, see for example [132].

**Complement 2.15** For an implementation of the assembly in Python, see script [assembly.py] [www.mathischeap.com/contents/LIBRARY/ptc/assembly](http://www.mathischeap.com/contents/LIBRARY/ptc/assembly).

Solving the global discrete linear system will give the coefficients of the weak solutions  $\mathbf{u}^h$  and  $\varphi^h$ ,

$$\left( \mathbf{u}^h, \varphi^h \right) \in \text{FP}_{N-1}(\Omega) \times \text{VP}_{N-1}(\Omega),$$

where in this case  $VP_{N-1}(\Omega) := \bigcup_{m=1}^{K^3} VP_{N-1}(\Omega_m)$  and  $FP_{N-1}(\Omega) := \bigcup_{m=1}^{K^3} FP_{N-1}(\Omega_m)$ .

**Complement 2.16** For a Python implementation of this particular example, see script [Poisson\_problem.py]  
[www.mathischeap.com/contents/LIBRARY/ptc/Poisson\\_problem](http://www.mathischeap.com/contents/LIBRARY/ptc/Poisson_problem).

### 2.4.3 Results

In Fig. 2.7, Some results of the eigen-spectrum of  $\mathbb{F}$ , the left-hand side matrix of the global system, are presented. It is shown that all eigenvalues are away from zero, which shows that the system is not singular. This is further supported by the results shown in Fig. 2.8 where condition numbers of  $\mathbb{F}$  under  $hp$ -refinement are presented.

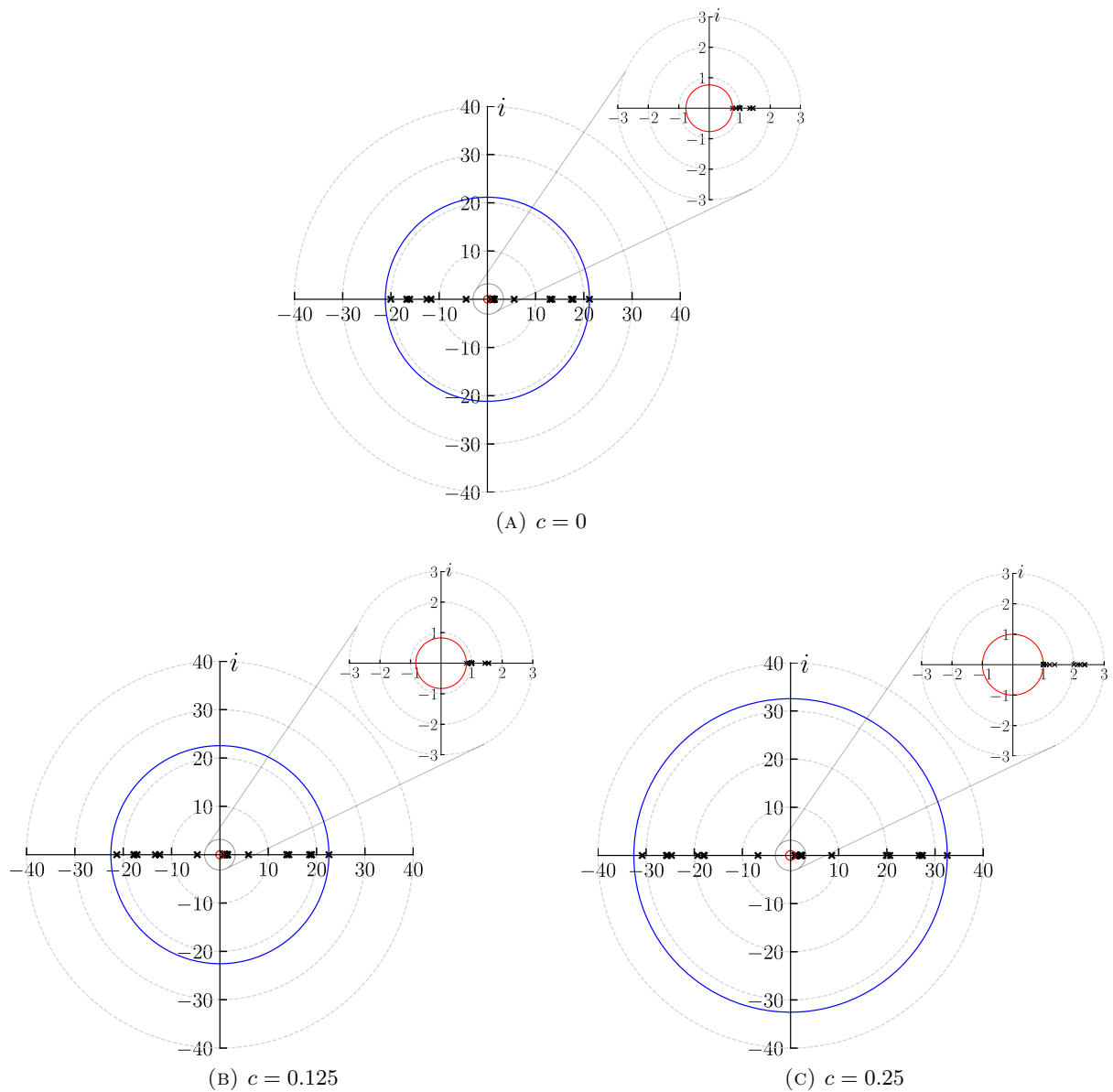


FIGURE 2.7: Results of the eigen-spectrum of  $\mathbb{F}$  for  $N = 1$ ,  $K = 2$ . The radii of the blue and red circles are the moduli of the eigenvalues of the maximum and minimum modulus respectively.

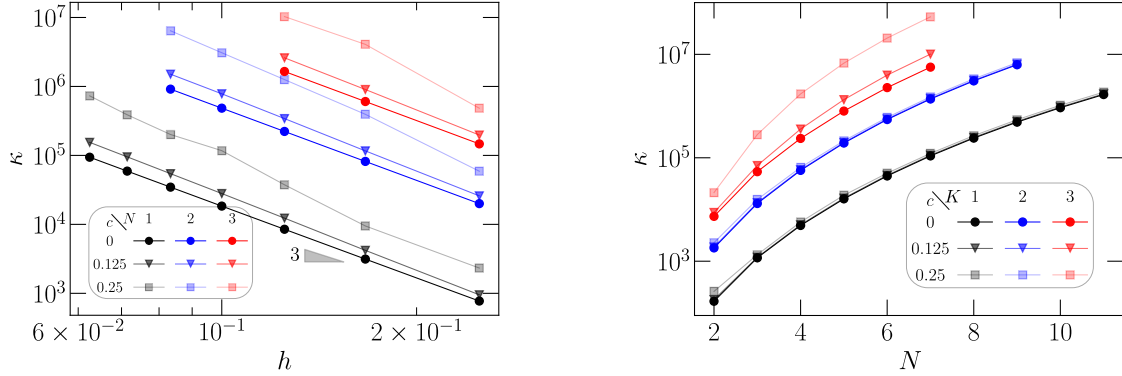


FIGURE 2.8: Condition numbers,  $\kappa$ , of  $\mathbb{F}$  under  $hp$ -refinement where  $h = \frac{1}{K}$  denotes the size of mesh cells.

We now investigate the accuracy of the MSEM. In Fig. 2.9, some results of the  $L^2$ - and  $H(\text{div})$ -error of the solution  $\mathbf{u}^h$  are presented. The  $\|\mathbf{u}^h\|_{H(\text{div})\text{-error}}$  is defined as

$$\|\mathbf{u}^h\|_{H(\text{div})\text{-error}} := \sqrt{\|\mathbf{u}^h\|_{L^2\text{-error}}^2 + \|\nabla \cdot \mathbf{u}^h\|_{L^2\text{-error}}^2}.$$

From these results, we can see that both  $\|\mathbf{u}^h\|_{L^2\text{-error}}$  and  $\|\mathbf{u}^h\|_{H(\text{div})\text{-error}}$  converge exponentially under  $p$ -refinement on either orthogonal ( $c = 0$ ) or curvilinear meshes ( $c > 0$ ). Similar exponential convergence is found for  $\varphi^h$  with respect to the  $L^2$ -error, see Fig. 2.10. These results correctly reflect the fact the MSEM is a spectral element method. The staircase-shaped convergence for  $c = 0$  and  $K = 1, 2$  is because in these cases some mimetic functions of particular degrees may miss some modes of the exact solution of  $f$  such that the projection error of  $f^h$ , see Fig. 2.11, converges in a staircase-shape. But, overall, this does not change the fact that the MSEM reduces the error of  $\mathbf{u}^h$  and  $\varphi^h$  exponentially under  $p$ -refinement.

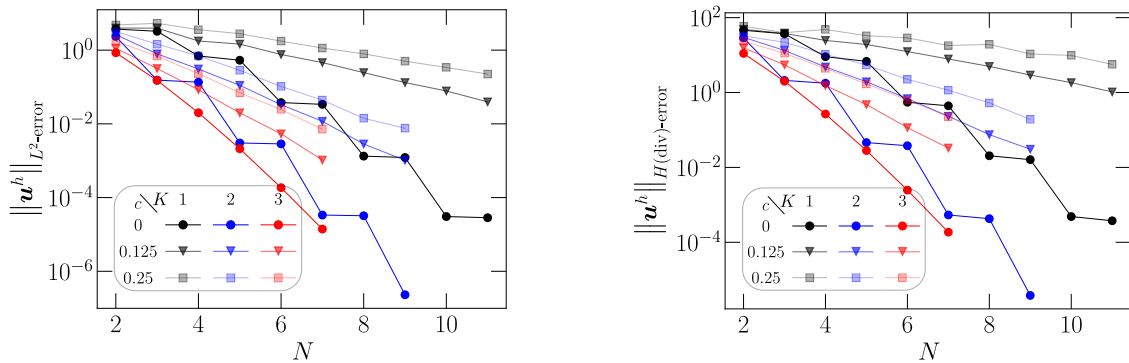
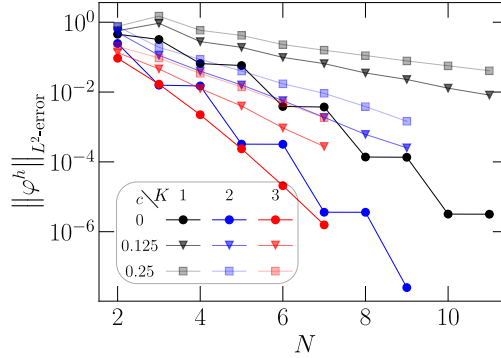
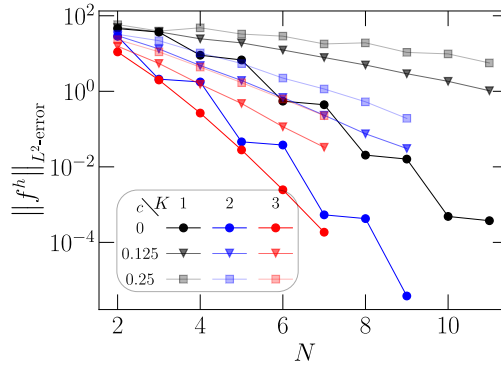
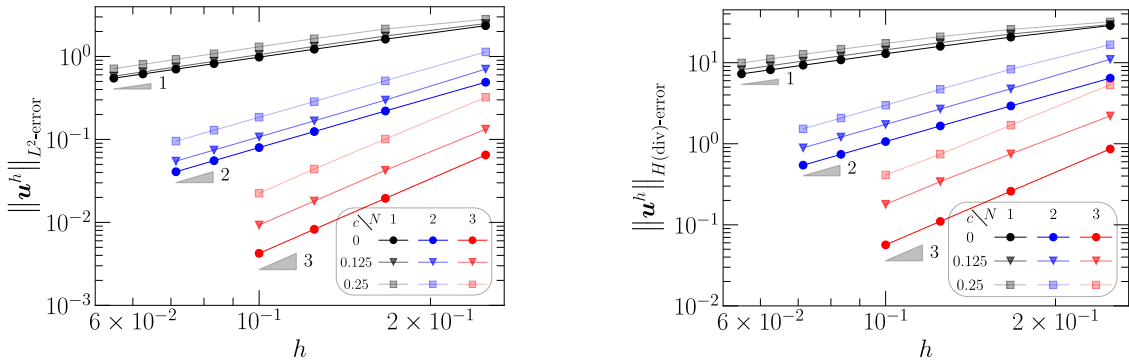


FIGURE 2.9: The convergence of  $\mathbf{u}^h$  with respect to  $L^2$ - and  $H(\text{div})$ -error under  $p$ -refinement.

In Fig. 2.12 where results of the  $L^2$ - and  $H(\text{div})$ -error of the solution  $\mathbf{u}^h$  under  $h$ -refinement are shown, we can see that both  $\|\mathbf{u}^h\|_{L^2\text{-error}}$  and  $\|\mathbf{u}^h\|_{H(\text{div})\text{-error}}$  always converge algebraically at the optimal rate on either orthogonal or curvilinear meshes. Similar results are found for the solution  $\varphi^h$  with respect to the  $L^2$ -error as shown in Fig. 2.13.

FIGURE 2.10: The convergence of  $\varphi^h$  with respect to  $L^2$ -error under  $p$ -refinement.FIGURE 2.11: The convergence of  $f^h$  with respect to the projection error,  $\|f^h - f\|_{L^2}$ , under  $p$ -refinement.FIGURE 2.12: Convergence of  $\mathbf{u}^h$  with respect to  $L^2$ - and  $H(\text{div})$ -error under  $h$ -refinement where  $h = \frac{1}{K}$  denotes the size of mesh cells.

We now investigate whether the conservation relation,  $\nabla \cdot \mathbf{u}^h = -f^h$  is preserved by the MSEM. In Fig. 2.14, the results of  $\|\nabla \cdot \mathbf{u}^h + f^h\|_{L^2}$  under  $hp$ -refinement are presented. From these results, we can conclude that the conservation relation,  $\nabla \cdot \mathbf{u}^h = -f^h$ , is always satisfied to machine precision ( $\mathcal{O}^{-13}$ ). The slight increasing of  $\|\nabla \cdot \mathbf{u}^h + f^h\|_{L^2}$  under  $p$ - or  $h$ -refinement is because of the increasing of the condition number when the size of the global system increases. In Fig. 2.15, we plot the local magnitude of  $\nabla \cdot \mathbf{u}^h + f^h$  on surfaces  $\hat{\Phi}([0, 1], [0, 1], 0.25)$  and

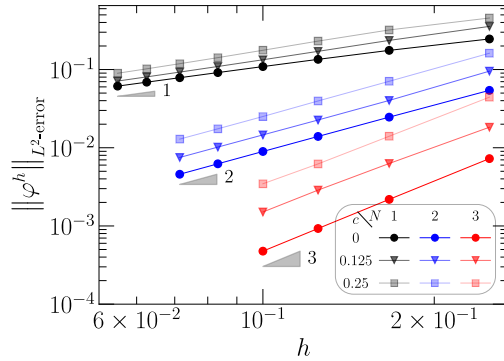


FIGURE 2.13: Convergence of  $\varphi^h$  with respect to  $L^2$ -error under  $h$ -refinement where  $h = \frac{1}{K}$  denotes the size of mesh cells.

$\mathring{\Phi}([0, 1], [0, 1], 0.75)$  in the computational domain for  $N = 4$  and  $K = 2$ . These results further support the claim that the MSEM preserves the conservation (divergence) relation of the Poisson problem. Note that this is only satisfied for  $f^h$  instead of  $f$ , which is understandable as in this manufactured case the term  $f$  is made of trigonometric functions, see (2.95), which can not be exactly represented by the mimetic functions of finite degree. For  $f$  that could be represented by finite degree mimetic functions (which usually is the case in practical problems like we set  $f = 0$  for conservation of mass in flow problems), we will have  $\nabla \cdot \mathbf{u}^h = -f^h = -f$ .

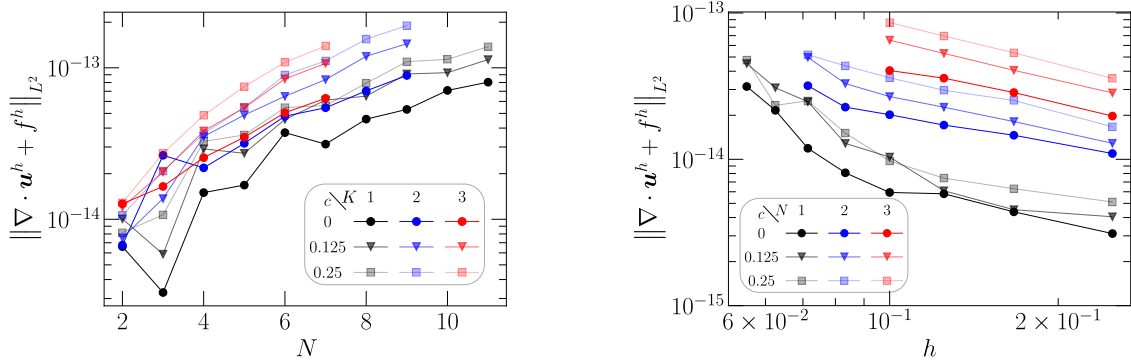


FIGURE 2.14: The  $L^2$ -norm of  $\nabla \cdot \mathbf{u}^h + f^h$  under  $hp$ -refinement where  $h = \frac{1}{K}$  denotes the size of mesh cells.

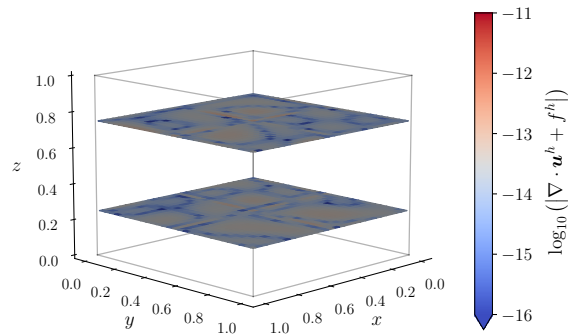
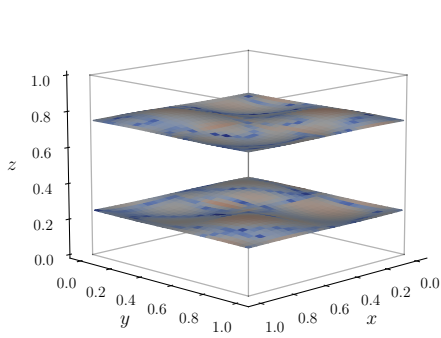
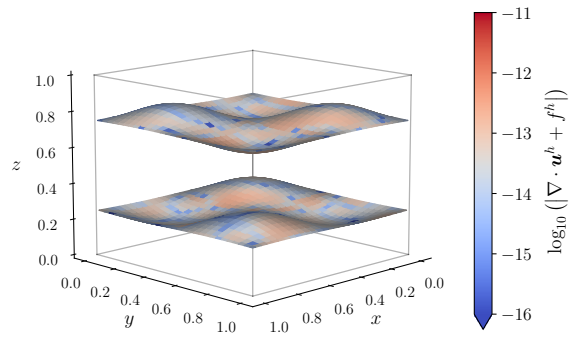
(A)  $c = 0$ (B)  $c = 0.125$ (C)  $c = 0.25$ 

FIGURE 2.15: Results of  $\log_{10}(|\nabla \cdot \mathbf{u}^h + f^h|)$  on mapped faces  $\mathring{\Phi}$  ( $\mathring{\Phi}([0, 1], [0, 1], 0.25)$  and  $\mathring{\Phi}([0, 1], [0, 1], 0.75)$ ), see (2.97), for  $N = 4$ ,  $K = 2$ .

BIBLIOGRAPHY

- [1] D. G. Gilbarg, N. S. Trudinger, *Elliptic Partial Differential Equations of Second Order*, 2001.
- [2] H. Brezis, *Functional Analysis, Sobolev Spaces and Partial Differential Equations*, 2011.
- [3] A. Palha, P. P. Rebelo, R. Hiemstra, J. Kreeft, M. Gerritsma, Physics-compatible discretization techniques on single and dual grids, with application to the Poisson equation of volume forms, *Journal of Computational Physics* 257 (2014) 1394–1422.
- [4] M. Gerritsma, A. Palha, V. Jain, Y. Zhang, Mimetic spectral element method for anisotropic diffusion, *SEMA SIMAI Springer Series* 15 (2018) 31–74.
- [5] K. Olesen, B. Gervang, J. N. Reddy, M. Gerritsma, A higher-order equilibrium finite element method, *Int J Numer Methods Eng.* 114 (2018) 1262–1290.
- [6] Y. Zhang, J. Fisser, M. Gerritsma, A hybrid mimetic spectral element method for three-dimensional linear elasticity problems, *Journal of Computational Physics* 433 (2021) 110179.
- [7] D. T. Blackstock, *Fundamentals of Physical Acoustics*, 2000.
- [8] A. Taflove, *Computational Electrodynamics: The Finite-Difference Time-Domain Method*, 1995.
- [9] M. Feit, J. Fleck, A. Steiger, Solution of the schrödinger equation by a spectral method, *Journal of Computational Physics* 47 (3) (1982) 412–433.
- [10] K. Hu, Y.-J. Lee, J. Xu, Helicity-conservative finite element discretization for incompressible MHD systems, *Journal of Computational Physics* 436 (2021) 110284.
- [11] K. Hu, J. Xu, Structure-preserving finite element methods for stationary MHD models, *Mathematics of Computation* 88 (316) (2018) 553–581.
- [12] J. Kreeft, M. Gerritsma, Mixed mimetic spectral element method for Stokes flow: A pointwise divergence-free solution, *Journal of Computational Physics* 240 (2013) 284–309.
- [13] M. Duponcheel, P. Orlandi, G. Winckelmans, Time-reversibility of the Euler equations as a benchmark for energy conserving schemes, *Journal of Computational Physics* 227 (2008) 8736–8752.
- [14] D. Lee, A. Palha, A mixed mimetic spectral element model of the 3D compressible Euler equations on the cubed sphere, *Journal of Computational Physics* 401 (2020) 108993.
- [15] H. K. Versteeg, W. Malalasekera, *An introduction to computational fluid dynamics : the finite volume method*, 2006.
- [16] A. Palha, M. Gerritsma, A mass, energy, enstrophy and vorticity conserving (MEEVC) mimetic spectral element discretization for the 2D incompressible Navier–Stokes equations, *Journal of Computational Physics* 328 (2017) 200–220.

- [17] Y. Zhang, A. Palha, M. Gerritsma, L. G. Rebholz, A mass-, kinetic energy- and helicity-conserving mimetic dual-field discretization for three-dimensional incompressible Navier-Stokes equations, part I: Periodic domains, *Journal of Computational Physics* (2021).
- [18] J. D. Anderson Jr, *Fundamentals of aerodynamics*, Tata McGraw-Hill Education, 2010.
- [19] F. P. Incropera, A. S. Lavine, T. L. Bergman, D. P. DeWitt, *Fundamentals of heat and mass transfer*, Wiley, 2007.
- [20] D. S. Jones, *The theory of electromagnetism*, Elsevier, 2013.
- [21] R. J. Blakely, *Potential theory in gravity and magnetic applications*, Cambridge university press, 1996.
- [22] A. M. Quarteroni, A. Valli, *Numerical Approximation of Partial Differential Equations*, Vol. 23, 2008.
- [23] D. P. Bertsekas, J. N. Tsitsiklis, *Parallel and Distributed Computation: Numerical Methods*, 1989.
- [24] G. D. Smith, *Numerical solution of partial differential equations : finite difference methods*, 1978.
- [25] T. J. Barth, D. C. Jespersen, The design and application of upwind schemes on unstructured meshes, in: *27th Aerospace Sciences Meeting*, 1989.
- [26] R. D. Cook, D. S. Malkus, M. E. Plesha, R. J. Witt, *Concepts and Applications of Finite Element Analysis*, 1974.
- [27] D. Boffi, F. Brezzi, M. Fortin, et al., *Mixed finite element methods and applications*, Vol. 44, Springer, 2013.
- [28] Y. Maday, A. T. Patera, Spectral element methods for the incompressible navier-stokes equations, in: *IN: State-of-the-art surveys on computational mechanics (A90-47176 21-64)*. New York, American Society of Mechanical Engineers, 1989, p. 71-143. Research supported by DARPA., 1989, pp. 71–143.
- [29] C. Canuto, M. Y. Hussaini, A. Quarteroni, A. Thomas Jr, et al., *Spectral methods in fluid dynamics*, Springer Science & Business Media, 2012.
- [30] C. Canuto, M. Y. Hussaini, A. Quarteroni, T. A. Zang, *Spectral methods: evolution to complex geometries and applications to fluid dynamics*, Springer Science & Business Media, 2007.
- [31] P. Bochev, A discourse on variational and geometric aspects of stability of discretizations, *33rd Computational Fluid Dynamics Lecture Series, VKI LS 5* (2003).
- [32] M. Gerritsma, Edge functions for spectral element methods, in: *Spectral and High Order Methods for Partial Differential Equations*, Springer, 2011, pp. 199–207.
- [33] A. Palha, High order mimetic discretization; development and application to laplace and advection problems in arbitrary quadrilaterals, Ph.D. thesis (2013).
- [34] J. Kreeft, Mimetic spectral element method; a discretization of geometry and physics, Ph.D. thesis (2013).
- [35] F. H. Harlow, J. E. Welch, Numerical calculation of time-dependent viscous incompressible flow of fluid with free surface, *The Physics of Fluids* 8 (1965) 2182.
- [36] J. Smagorinsky, General circulation experiments with the primitive equations. I.: The basic experiment, *Monthly weather Review* 91 (1963) 99–164.
- [37] D. K. Lilly, On the application of the eddy viscosity concept in the internal subrange of turbulence, *NCAR Manuscript* (1966) 123.
- [38] E. Tonti, On the mathematical structure of a large class of physical theories (1971).
- [39] E. Tonti, The algebraic-topological structure of physical theories (1974) 441–467.
- [40] E. Tonti, On the formal structure of physical theories, 1975.
- [41] E. Tonti, The reason for analogies between physical theories, *Applied Mathematical Modelling* 1 (1) (1976) 37–50.

- [42] A. Dold, Lectures on Algebraic Topology, 1972.
- [43] A. Hatcher, Algebraic topology, 2001.
- [44] R. Bott, L. W. Tu, Differential Forms in Algebraic Topology, 1982.
- [45] J. M. Lee, Introduction to Smooth Manifolds, 2002.
- [46] T. Frankel, The Geometry of Physics: An Introduction, 2012.
- [47] J. B. Perot, C. J. Zusi, Differential forms for scientists and engineers, *Journal of Computational Physics* 257 (2014) 1373–1393.
- [48] E. Tonti, Why starting from differential equations for computational physics, *Journal of Computational Physics* 257 (2014) 1260–1290.
- [49] E. Tonti, The Mathematical Structure of Classical and Relativistic Physics, 2013.
- [50] H. Whitney, Geometric Integration Theory, 1957.
- [51] J. Dodziuk, Finite-difference approach to the hodge theory of harmonic forms, *American Journal of Mathematics* 98 (1) (1976) 79.
- [52] J. Lohi, L. Kettunen, Whitney forms and their extensions, *Journal of Computational and Applied Mathematics* 393 (2021) 113520.
- [53] F. Brezzi, On the existence, uniqueness and approximation of saddle-point problems arising from Lagrangian multipliers, *Revue française d’automatique, informatique, recherche opérationnelle. Analyse numérique* 8 (2) (1974) 129–151.
- [54] P. A. Raviart, J. M. Thomas, A mixed finite element method for 2nd order elliptic problems, *Mathematical Aspects of the Finite Element Method, Lecture Notes in Mathematics* 606 (1977) 292–315.
- [55] J. C. Nédélec, Mixed finite elements in  $\mathbb{R}^3$ , *Numer. Math.* 35 (1980) 315–341.
- [56] F. Brezzi, J. Douglas, L. D. Marini, Two families of mixed finite elements for second order elliptic problems, *Numerische Mathematik* 47 (2) (1985) 217–235.
- [57] J. C. Nédélec, A new family of mixed finite elements in  $\mathbb{R}^3$ , *Numer. Math.* 50 (1) (1986) 57–81.
- [58] A. Bossavit, Whitney forms: a class of finite elements for three-dimensional computations in electromagnetism, *IEE Proceedings A Physical Science, Measurement and Instrumentation, Management and Education, Reviews* 135 (8) (1988) 493–500.
- [59] A. Bossavit, Mixed finite elements and the complex of Whitney forms, *The mathematics of finite elements and applications VI* (1988) 137–144.
- [60] A. Bossavit, A rationale for “edge-elements” in 3-D fields computations, *IEEE Transactions on Magnetism* 24 (1) (1988) 74–79.
- [61] A. Bossavit, I. Mayergoyz, Edge-elements for scattering problems, *IEEE Transactions on Magnetism* 25 (4) (1989) 2816–2821.
- [62] A. Bossavit, Solving maxwell equations in a closed cavity, and the question of ‘spurious modes’, *IEEE Transactions on Magnetism* 26 (2) (1990) 702–705.
- [63] A. Bossavit, Generating Whitney forms of polynomial degree one and higher, *IEEE Transactions on Magnetism* 38 (2) (2002) 341–344.
- [64] F. Rapetti, High order edge elements on simplicial meshes, *Mathematical Modelling and Numerical Analysis* 41 (6) (2007) 1001–1020.
- [65] A. Bossavit, A uniform rationale for Whitney forms on various supporting shapes, *Mathematics and Computers in Simulation* 80 (8) (2010) 1567–1577.
- [66] A. Bossavit, Computational electromagnetism and geometry: Building a finite-dimensional “Maxwell’s house” (1): Network equations, *Applied and Environmental Microbiology* 7 (2) (1999) 150–159.
- [67] A. Bossavit, Computational electromagnetism and geometry: (2): Network constitutive laws, *Applied and Environmental Microbiology* 7 (3) (1999) 294–301.

- [68] A. Bossavit, Computational electromagnetism and geometry: (3): Convergence, *Applied and Environmental Microbiology* 7 (4) (1999) 401–408.
- [69] A. Bossavit, Computational electromagnetism and geometry: (4): From degrees of freedom to fields, *Applied and Environmental Microbiology* 8 (1) (2000) 102–109.
- [70] A. Bossavit, Computational electromagnetism and geometry: (5): The "Galerkin hodge", *Applied and Environmental Microbiology* 8 (2) (2000) 203–209.
- [71] A. Bossavit, A new viewpoint on mixed elements, *Meccanica* 27 (1) (1992) 3–11.
- [72] K. Lipnikov, G. Manzini, M. Shashkov, Mimetic finite difference method, *Journal of Computational Physics* 257 (2014) 1163–1227.
- [73] J. M. Hyman, J. C. Scovel, Deriving mimetic difference approximations to differential operators using algebraic topology, Los Alamos National Laboratory (1988).
- [74] M. Shashkov, *Conservative Finite-Difference Methods on General Grids*, 1996.
- [75] J. Hyman, M. Shashkov, S. Steinberg, The numerical solution of diffusion problems in strongly heterogeneous non-isotropic materials, *Journal of Computational Physics* 132 (1) (1997) 130–148.
- [76] J. Hyman, M. Shashkov, Natural discretizations for the divergence, gradient, and curl on logically rectangular grids, *Computers & Mathematics With Applications* 33 (4) (1997) 81–104.
- [77] J. Hyman, M. Shashkov, Approximation of boundary conditions for mimetic finite-difference methods, *Computers & Mathematics With Applications* 36 (5) (1998) 79–99.
- [78] J. Hyman, M. Shashkov, S. Steinberg, The effect of inner products for discrete vector fields on the accuracy of mimetic finite difference methods, *Computers & Mathematics With Applications* 42 (12) (2001) 1527–1547.
- [79] K. Lipnikov, M. Shashkov, D. Svyatskiy, The mimetic finite difference discretization of diffusion problem on unstructured polyhedral meshes, *Journal of Computational Physics* 211 (2) (2006) 473–491.
- [80] L. Beir, F. Brezzi, S. Arabia, Basic principles of virtual element methods, *Mathematical Models and Methods in Applied Sciences* 23 (1) (2013) 199–214.
- [81] M. F. Benedetto, S. Berrone, A. Borio, S. Pieraccini, S. Scialò, A hybrid mortar virtual element method for discrete fracture network simulations, *Journal of Computational Physics* 306 (2016) 148–166.
- [82] P. Korn, L. Linardakis, A conservative discretization of the shallow-water equations on triangular grids, *Journal of Computational Physics* 375 (2018) 871–900.
- [83] P. B. Bochev, J. M. Hyman, Principles of mimetic discretizations of differential operators, in: *Compatible spatial discretizations*, Springer, 2006, pp. 89–119.
- [84] A. N. Hirani, *Discrete Exterior Calculus*, Ph.D. thesis (2003).
- [85] M. Desbrun, A. N. Hirani, M. Leok, J. E. Marsden, Discrete exterior calculus, *Arxiv preprint math0508341* (2005).
- [86] A. N. Hirani, K. Kalyanaraman, E. B. Vanderzee, Delaunay Hodge star, *CAD Computer Aided Design* 45 (2) (2013) 540–544.
- [87] M. S. Mohamed, A. N. Hirani, R. Samtaney, Discrete exterior calculus discretization of incompressible Navier-Stokes equations over surface simplicial meshes, *Journal of Computational Physics* 312 (2016) 175–191.
- [88] N. Robidoux, S. Steinberg, A discrete vector calculus in tensor grids, *Computational methods in applied mathematics* 11 (1) (2011) 23–66.
- [89] B. Perot, Conservation properties of unstructured staggered mesh schemes, *Journal of Computational Physics* 159 (1) (2000) 58–89.

- [90] X. Zhang, D. Schmidt, B. Perot, Accuracy and conservation properties of a three-dimensional unstructured staggered mesh scheme for fluid dynamics, *Journal of Computational Physics* 175 (2) (2002) 764–791.
- [91] D. N. Arnold, R. S. Falk, R. Winther, Differential complexes and stability of finite element methods. I. The de Rham complex (2006) 23–46.
- [92] D. N. Arnold, R. S. Falk, R. Winther, Differential complexes and stability of finite element methods II: The elasticity complex (2006) 47–67.
- [93] D. N. Arnold, R. S. Falk, R. Winther, Finite element exterior calculus, homological techniques, and applications, *Acta Numerica* 15 (2006) 1–155.
- [94] D. N. Arnold, R. S. Falk, R. Winther, Finite element exterior calculus: From Hodge theory to numerical stability, *Bulletin of the American Mathematical Society* 47 (2) (2010) 281–354.
- [95] J. A. Evans, T. J. R. Hughes, Isogeometric divergence-conforming B-splines for the steady Navier-Stokes equations, *Mathematical Models and Methods in Applied Sciences* 23 (8) (2013) 1421–1478.
- [96] D. Toshniwal, T. J. Hughes, Isogeometric discrete differential forms: Non-uniform degrees, Bézier extraction, polar splines and flows on surfaces, *Computer Methods in Applied Mechanics and Engineering* 376 (2021) 113576.
- [97] R. Hiptmair, Canonical construction of finite elements, *Mathematics of Computation* 68 (228) (1999) 1325–1346.
- [98] R. Hiptmair, Discrete hodge-operators: an algebraic perspective, *Progress in Electromagnetics Research-pier* 32 (2001) 247–269.
- [99] J. Bonelle, A. Ern, Analysis of compatible discrete operator schemes for elliptic problems on polyhedral meshes, *Mathematical Modelling and Numerical Analysis* 48 (2) (2014) 553–581.
- [100] J. Bonelle, A. Ern, Analysis of compatible discrete operator schemes for the stokes equations on polyhedral meshes, *Ima Journal of Numerical Analysis* 35 (4) (2015) 1672–1697.
- [101] D. A. D. Pietro, A. Ern, A family of arbitrary-order mixed methods for heterogeneous anisotropic diffusion on general meshes (2013).
- [102] E. Hairer, C. Lubich, G. Wanner, Geometric numerical integration illustrated by the störmer-verlet method, *Acta Numerica* 12 (2003) 399–450.
- [103] E. Hairer, C. Lubich, G. Wanner, Geometric numerical integration: structure-preserving algorithms for ordinary differential equations, Vol. 31, Springer Science & Business Media, 2006.
- [104] E. Hairer, C. Lubich, G. Wanner, Geometric Numerical Integration: Structure-Preserving Algorithms for Ordinary Differential Equations, 2009.
- [105] D. Furihata, T. Matsuo, Discrete Variational Derivative Method: A Structure-Preserving Numerical Method for Partial Differential Equations, 2010.
- [106] D. Furihata, S. Sato, T. Matsuo, A novel discrete variational derivative method using “average-difference methods”, *JSIAM Letters* 8 (2015) 81–84.
- [107] M. C. Pinto, K. Kormann, E. Sonnendrücker, Variational framework for structure-preserving electromagnetic particle-in-cell methods., arXiv preprint arXiv:2101.09247 (2021).
- [108] T. C. Ionescu, A. Astolfi, Families of moment matching based, structure preserving approximations for linear port hamiltonian systems, *Automatica* 49 (8) (2013) 2424–2434.
- [109] A. Palha, M. Gerritsma, Mimetic spectral element method for hamiltonian systems, arXiv preprint arXiv:1505.03422 (2015).
- [110] L. B. da Veiga, L. Lopez, G. Vacca, Mimetic finite difference methods for Hamiltonian wave equations in 2d, *Computers & Mathematics With Applications* 74 (5) (2017) 1123–1141.

- [111] N. Liu, Y. Wu, Y. L. Gorrec, H. Ramirez, L. Lefèvre, Structure-preserving discretization and control of a two-dimensional vibro-acoustic tube, *Ima Journal of Mathematical Control and Information* 38 (2) (2021) 417–439.
- [112] J. Kreeft, A. Palha, M. Gerritsma, Mimetic framework on curvilinear quadrilaterals of arbitrary order, arXiv preprint arXiv:1111.4304 (2011).
- [113] M. Gerritsma, An introduction to a compatible spectral discretization method, *Mechanics of Advanced Materials and Structures* 19 (1) (2012) 48–67.
- [114] R. Hiemstra, D. Toshniwal, R. Huijsmans, M. Gerritsma, High order geometric methods with exact conservation properties, *Journal of Computational Physics* 257 (2014) 1444–1471.
- [115] A. Palha, B. Koren, F. Felici, A mimetic spectral element solver for the grad-shafranov equation, *Journal of Computational Physics* 316 (2016) 63–93.
- [116] D. Lee, A. Palha, A mixed mimetic spectral element model of the rotating shallow water equations on the cubed sphere, *Journal of Computational Physics* 375 (2018) 240–262.
- [117] Y. Zhang, V. Jain, A. Palha, M. Gerritsma, The discrete Steklov–Poincaré operator using algebraic dual polynomials, *Computational Methods in Applied Mathematics* 19 (3) (2019) 645–661.
- [118] Y. Zhang, V. Jain, A. Palha, M. Gerritsma, Discrete equivalence of adjoint Neumann–Dirichlet div-grad and grad-div equations in curvilinear 3D domains, *Lecture Notes in Computational Science and Engineering* 134 (2020) 203–213.
- [119] M. Gerritsma, V. Jain, Y. Zhang, A. Palha, Algebraic dual polynomials for the equivalence of curl-curl problems, *Lecture Notes in Computational Science and Engineering* 132 (2020) 307–320.
- [120] R. A. Adams, J. J. Fournier, *Sobolev spaces*, Elsevier, 2003.
- [121] S. Brenner, R. Scott, *The mathematical theory of finite element methods*, Vol. 15, Springer Science & Business Media, 2007.
- [122] V. Girault, P.-A. Raviart, *Finite Element Methods for Navier-Stokes Equations: Theory and Algorithms*, 1986.
- [123] C. Carstensen, L. Demkowicz, J. Gopalakrishnan, Breaking spaces and forms for the dpg method and applications including maxwell equations, *Computers & Mathematics With Applications* 72 (3) (2016) 494–522.
- [124] T. J. Willmore, *An introduction to differential geometry*, Courier Corporation, 2013.
- [125] T. Frankel, *The geometry of physics: an introduction*, Cambridge university press, 2011.
- [126] D. N. Arnold, R. S. Falk, R. Winther, Differential complexes and stability of finite element methods i. the de Rham complex, in: *Compatible spatial discretizations*, Springer, 2006, pp. 23–46.
- [127] D. N. Arnold, Spaces of finite element differential forms, in: *Analysis and numerics of partial differential equations*, Springer, 2013, pp. 117–140.
- [128] A. Buffa, G. Sangalli, J. Rivas, R. Vazquez, Isogeometric discrete differential forms in three dimensions, *SIAM J. Numer. Anal.* 118 (2011) 271–844.
- [129] A. Ratnani, E. Sonnendrücker, An arbitrary high-order spline finite element solver for the time domain Maxwell equations, *Journal of Scientific Computing* (2012) 87–106.
- [130] Y. Zhang, V. Jain, A. Palha, M. Gerritsma, The use of dual B-spline representations for the double de Rham complex of discrete differential forms, *Lecture Notes in Computational Science and Engineering* 133 (2021) 227–242.
- [131] S. Steinberg, *Fundamentals of grid generation*, CRC press, 1993.
- [132] F. Cuvelier, C. Japhet, G. Scarella, An efficient way to assemble finite element matrices in vector languages, *BIT Numerical Mathematics* 56 (3) (2016) 833–864.